

# Partially Hidden Markov Chain Linear Autoregressive model: inference and forecasting

Fatoumata Dama<sup>†</sup> and Christine Sinoquet<sup>†</sup>

<sup>†</sup>LS2N / UMR CNRS 6004, Nantes University, France  
`{fatoumata.dama, christine.sinoquet}@univ-nantes.fr`

## Abstract

Time series subject to change in regime have attracted much interest in domains such as econometry, finance or meteorology. For discrete-valued regimes, some models such as the popular Hidden Markov Chain (HMC) describe time series whose state process is *unknown* at all time-steps. Sometimes, time series are firstly labelled thanks to some annotation function. Thus, another category of models handles the case with regimes *observed* at all time-steps. We present a novel model which addresses the intermediate case: (i) state processes associated to such time series are modelled by Partially Hidden Markov Chains (PHMCs); (ii) a linear autoregressive (LAR) model drives the dynamics of the time series, within each regime. We describe a variant of the expectation maximization (EM) algorithm devoted to PHMC-LAR model learning. We propose a hidden state inference procedure and a forecasting function that take into account the observed states when existing. We assess inference and prediction performances, and analyze EM convergence times for the new model, using simulated data. We show the benefits of using partially observed states to decrease EM convergence times. A fully labelled scheme with unreliable labels also speeds up EM. This offers promising prospects to enhance PHMC-LAR model selection. We also point out the robustness of PHMC-LAR to labelling errors in inference task, when large training datasets and moderate labelling error rates are considered. Finally, we highlight the remarkable robustness to error labelling in the prediction task, over the whole range of error rates.

**Keywords** Time series analysis . Autoregressive model . Regime-switching model . Markov chain . Forecasting . Hidden state inference

## 1 Introduction

Time series are widely present in many domains such as industry, energy, meteorology, e-commerce, social networks or health. They represent the temporal evolving of systems and help us to understand their temporal dynamics and perform short-, medium- or long-term predictions. A major research line has been dedicated to time series analysis. In this line, exponential smoothing models (Gardner Jr and Everette, 2006; Bergmeir et al., 2016), Box and Jenkins models (Box et al., 2015) and nonlinear autoregressive neural networks (Yu et al., 2014; Wang et al., 2019; Noman et al., 2020) are essentially devoted to forecasting. In addition to the forecasting goal, regime-switching autoregressive models (Ubilava and Helmers, 2013; Hamilton, 1990) also allow to discover hidden behaviors of such systems.

In the cases when the studied system is **stationary**, that is its behavior is time-independent, the Linear Autoregressive (LAR) model is a framework widely used to capture the autoregressive dynamics of the corresponding time series (Wold, 1954; Degtyarev and Gankevich, 2019). The LAR model is a simple linear regression model in which predictors are lagged values of the current value in the time series. However, many real-life systems are subject to changes in behaviors: for instance in econometry, we distinguish between recession and expansionary phases; in meteorology, anticyclonic conditions alternate with low pressure conditions. These systems are commonly referred to as **regime-switching systems**, where each regime corresponds to a specific behavior. Each time-step is associated with some state, amongst those allowed for the system. Regime-switching system modelling is achieved in two steps: (i) the state process modelling that enables to capture how states are generated, and (ii) the modelling of the autoregressive dynamics of the time series within each regime. In the latter step, a simple autoregressive framework such as the LAR model can be used. Generally, in step (i), the state process is modelled by a **discrete-valued Markov process**. In the current state-of-the-art literature, two categories of models can be distinguished.

In **Hidden Regime-Switching Autoregressive (HRSAR) models**, the state process is hidden and is modelled by a Hidden Markov Process (HMP). This category of models has been introduced by [Hamilton \(1989\)](#) in the context of United States’s Gross National Product time series analysis. Several variants and extensions were subsequently designed.

In **Observed Regime-Switching Autoregressive (ORSAR) models**, the state process is either observed or derived *a priori*. In the latter case, a clustering algorithm is used before fitting the model, to extract the regimes. The clustering may either rely on endogenous variables (*i.e.*, the variables whose dynamics is observed through the time series) or on exogenous variables supposed to drive regime-switching. The recent work of [Bessac, Ailliot, Cattiaux, and Monbet \(2016\)](#) illustrates the application of these models to wind time series.

When the state process is partially observed, which means that the system state is known at some random time-steps and unknown for the remaining time-steps, ORSAR models cannot be directly applied while HRSAR models are suboptimal in the sense that the observed states cannot be included.

To overcome these limitations, in this work, we propose a novel **regime-switching autoregressive** model that capitalizes on the observed states while the hidden states are inferred. We consider a special case of Markov process henceforth named **Markov Chain**. Our model is referred to as the Partially Hidden Markov Chain Linear AutoRegressive (PHMC-LAR) model. The PHMC-LAR model is a flexible parametric model that supplies a unification of HRSAR and ORSAR models when the state process is a Markov Chain. Thus, when the state process is fully observed, PHMC-LAR is reduced to ORSAR. Reversely, when the state process is fully hidden, PHMC-LAR instantiates as HRSAR. Beyond the unification aspect, we contribute to the machine learning literature through designing the underlying algorithmic machinery dedicated to effective and efficient PHMC-LAR model training.

The main contributions of this paper are as follows:

1. We propose a new regime-switching autoregressive model that integrates the states observed at some random time-steps. This model, referred to as PHMC-LAR, provides a unification of HRSAR and ORSAR models when the state process is modelled by a Markov Chain (MC).
2. We propose a variant of the **Expectation-Maximization (EM) algorithm** that allows to learn the parameters of our model.
3. Inference on hidden states is carried out by a variant of the **Viterbi algorithm**, adapted to take into account the observed states.
4. Regarding the time series forecasting task, a prediction function is proposed. We distinguish between the case where the system state is known at forecast horizons from the case where it is latent.

The ability of our model to infer the hidden states and to make accurate predictions on time series, even when the observed states are unreliable, is investigated through experiments performed on synthetic data. Our work underlines the benefits of using partially observed states to decrease EM convergence times. This performance is obtained with no or practically no impact on the quality of hidden state inference, as from labelling percentages around 20%-30%; the prediction accuracy is also preserved above such percentage thresholds. For instance, for a training set of 100 sequences, with 70% labelled states, the EM algorithm converges after 22 iterations on average against 62 on average for the unsupervised case. Moreover, performing fully supervised training with a proportion of ill-labelled states is also beneficial for EM convergence. For example, given a training set of size 100 annotated with a 70%-reliable labelling function, the EM algorithm converges after a single iteration against 67 iterations for the unsupervised case. This offers promising prospects to enhance model selection for the PHMC-LAR model. Further experimentations also show the ability of our variant of the Viterbi algorithm to infer hidden states in partially-labelled sequences. In addition, while assessing the impact on predictions generated by incorporating labelled states in the training sequences, we also compared the situations where all states are unknown at forecast horizons to the situations where all states are known. Prediction errors are subdued at all horizons in the latter case (by 44% on average), but contrasted horizons are still evidenced with low (respectively high) scores as in the former case. The contrast is kept constant whatever the percentage of observed states in the training set. Besides, we also point out the robustness of our model to labelling errors in inference task, when large training datasets and moderate labelling error rates are considered. Finally, the latter experiment highlights the remarkable robustness to error labelling in the prediction task, over the whole range of error rates.

This paper is organized as follows. Related work is reviewed in Section 2. Section 3 describes the PHMC-LAR model. Then a learning algorithm is derived in Section 4, to estimate the model parameters. Inference of the hidden states is addressed in Section 5. Section 6 presents the time series forecasting procedure. Section 7 depicts the experimental protocol that drove our experimentations on synthetic data, and discusses the results obtained. Section 8 concludes this paper.

## 2 Related work

This section first highlights the links between our proposal, PHMC-LAR, and the most closely related contributions of the literature. The PHMC-LAR combines a variant of the Hidden Markov Model (HMM), namely the Partially Hidden Markov Chain (PHMC), with the Linear AutoRegressive (LAR) model. The rest of this section reviews the two main models that compose the hybrid model proposed.

As mentioned in the introduction, the PHMC-LAR model unifies the HRSAR and ORSAR frameworks. However, the common thread between these latter frameworks is the implication of dependencies that drive the local dynamics within each regime. Therefore, the contributions of the literature most closely related to PHMC-LAR are also characterized by various local dynamics.

Several models closely related to HRSAR were proposed in the literature. The MS-AR model (Markov-switching AutoRegressive model) designed by [Hamilton \(1989\)](#) combines ARIMA (AutoRegressive Integrated Moving Average) models with an HMM, to characterize changes in the parameters of an autoregressive process. The targeted application motivating the MS-AR model was economic analysis: the switch between fast growth and slow growth is governed by the outcome of the Markov process.

Further, [Filardo \(1994\)](#) incorporated time-varying transition probabilities between regimes in the MS-AR model. For instance, the resulting model was subsequently used to reproduce the cyclic patterns existing in climatic variables ([Cardenas-Gallo et al., 2016](#)). In parallel, the Hamilton’s MS-AR model was also extended into a general dynamic linear model combined with Markov-switching ([Kim, 1994](#)). Finally, Michalek and co-authors’ work focused on a HRSAR model that integrates HMM with Moving Average (MA) models ([Michalek et al., 2000](#)). In the same work, the parameter estimation approximation thus derived was generalized to deal with AutoRegressive Moving Average (ARMA) hybridized with HMM. Simulations of electrophysiological recordings showed that the derived estimators allow to recover the true dynamics where standard HMM fails. The model generalized by Michalek and collaborators, to integrate HMM with ARMA, was also applied to model human activity as time signals for activity early recognition ([Li and Fu, 2012](#)).

More recently, a nonhomogeneous HRSAR model was developed to model wind time series ([Ailliot et al., 2015](#)). The aim was to acknowledge that the probability of switching from cyclonic conditions to anticyclonic conditions between time-steps  $t$  and  $t + 1$  depends on the wind conditions at time-step  $t$  at some given location off the French Brittany coast. A nonhomogeneous MS-AR (NHMS-AR) model was thus designed for this purpose.

To our knowledge, the investigations around ORSAR models are limited to the recent work of [Bessac, Ailliot, Cattiaux, and Monbet \(2016\)](#) which was applied to wind time series. Therein, observed regimes are derived by running a clustering procedure on the variables under study or on extra variables. Thus are identified the states, all distinct from one other, in which the data are homogeneous. Besides comparing the ORSAR models derived from various clustering procedures, Bessac and collaborators also compare the respective merits of HRSAR and ORSAR models on real-world and simulated data.

### 2.1 Partially Hidden Markov Chain - PHMC( $K$ )

Hidden Markov models (HMMs) have been successfully used in such domains as natural language processing ([Morwal et al., 2012](#)), handwriting recognition ([Mouhcine et al., 2018](#)), speech emotion recognition ([Schuller et al., 2003](#)), human action recognition ([Berg et al., 2018](#)) or renewable power prediction ([Ghasvarian Jahromi et al., 2020](#)), to name but a few.

HMM( $K$ ) is a flexible probabilistic *framework* able to model complex hidden-regime-switching systems. It exactly possesses  $K$  states where each state drives the specific behavior of an observed variable. This variable is itself modelled through a usual probability law such as a Gaussian law, for example. The system state process, which specifies the ongoing behavior of the latter observed variable at each time-step, is fully latent. Therefore, state inference is the main purpose of HMM models: the goal is to learn about the latent sequence of states from the observed behavior. This task is generally driven by Maximum A Posteriori (MAP) estimation implemented through the **Viterbi algorithm** ([Forney, 1973](#)). Importantly, the HMM framework satisfies the Markov property, which stipulates that the conditional probability distribution of the hidden state at time-step  $t$ , given the hidden states at previous time-steps  $t' < t$ , only depends on the hidden state at time-step  $t - 1$ . Besides, the observed behavior at time-step  $t$  solely depends on the hidden variable at time-step  $t$ .

When dealing with systems in which the state process is partially observed or known, applying HMM would result in an important information loss in the sense that the observed states are ignored. To overcome this limitation, [Scheffer and Wrobel \(2001\)](#) have introduced the Partially Hidden Markov Chain (PHMC), which integrates partially observed states in the modelling process. The authors have proposed an active learning algorithm in which the user is asked to label difficult observations identified during model learning. More recently, [Ramasso and Denoeux](#)

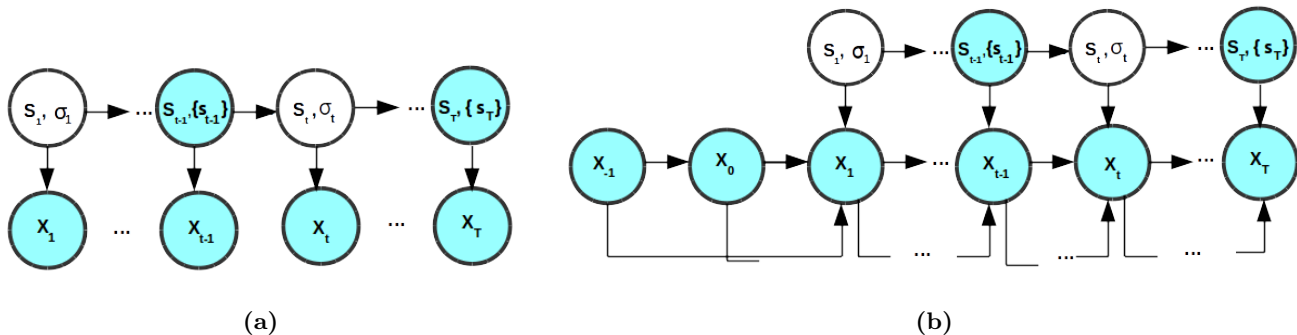


**Figure 1** The conditional independence graphs of the Partially Hidden Markov Chain and of the Partially Hidden Markov Chain Linear Autoregressive (PHMC-LAR) model, when the LAR order  $p$  is equal to 2. (a) PHMC model. (b) PHMC-LAR model. Observed states are shown in dark shade whereas hidden states are colored in light shade. When a state is observed,  $\sigma_t$  is reduced to a singleton.

(2013) have proposed a model that makes use of partial knowledge on HMM states. These authors have modelled the partial knowledge by a *belief function* that specifies the probability of each state at each time-step. The works carried out by Ramasso and Denoeux (2013) have shown that the use of partial knowledge on states accelerates HMM model learning.

## 2.2 Linear AutoRegressive model - LAR( $p$ )

An observed time series is considered to be one realization of a stochastic process. Time series analysis and forecasting thus require that the underlying stochastic process be modelled. The linear autoregressive (LAR) model is a stochastic model widely used for this purpose. A LAR model of order  $p$  is a linear model in which the regressors are the  $p$  past values of the variable, hence the term autoregression. Although the LAR model is conceptually simple and easy to learn, it can only be applied to **stationary time series**. When this condition is violated, *model misspecification* issues arise. Nonetheless, it is well known that if the autoregressive coefficients of a LAR process are all less than one in module, then the process will be stationary. This is a necessary and sufficient condition which is tested through **unit root tests** (Phillips and Perron, 1988; Dickey and Fuller, 1979; Kwiatkowski et al., 1992).

In the LAR( $p$ ) model, the hyper-parameter  $p$  denotes the number of past observations to include in the prediction at time-step  $t$ . Two alternative methods are generally used to fix the value of  $p$ . The first one relies on a well-known property of the *partial autocorrelation function* of the LAR( $p$ ) model: the autocorrelation becomes null from lag  $p+1$ . The second method, more general, tests a range of candidate values for  $p$ , then selects the value that minimizes a model selection criterion such as the Bayesian information criterion (BIC) or the Akaike's information criterion (AIC).

## 3 The PHMC-LAR model

In this section, we explain how we have created a new regime-switching model called PHMC-LAR, based on the PHMC and LAR models. The section first introduces some notations. Then Subsection 3.2 describes our proposal to model the state process by a PHMC model. Subsection 3.3 details how, within each regime, the dynamics of the observed variable is governed by a LAR model. Thus, the bivariate process follows a PHMC-LAR model.

To note, the fundamental difference between our model and the two other approaches identified in the same line Scheffer and Wrobel (2001); Ramasso and Denoeux (2013) is the autoregressive dynamics of our model (see Fig. 1).

### 3.1 Notations

- Symbol  $:=$  stands for the *definition symbol*.
- $\mathbf{1}_A : \Omega \rightarrow \{0, 1\}$  denotes the *indicator function* that indicates membership of an element in a subset  $A$  of  $\Omega$ . As from now,  $\mathbf{1}_A$  will be noted  $\mathbf{1}_{\{x \in A\}}$ .
- $\{X_t\}_{t \in \mathbb{Z}}$  denotes a stochastic process. By convention,  $X_{1-p}^0$  denotes the  $p$  initial values of the time series  $\{X_t\}$ . For each  $t \geq 1$ ,  $X_{t-p}^{t-1}$  stands for the subseries  $\{X_{t-p}, X_{t-p+1} \cdots X_{t-1}\}$ .

- $\mathbf{x} = x_1^T$  represents an observed time series with  $\mathbf{x}_0 = x_{1-p}^0$  the corresponding initial values.
- $\{S_t\}_{t \in \mathbb{N}^*}$  denotes a state process depicting the temporal evolution of a regime-switching system where the set of states is  $\mathbf{K} = \{1, 2, \dots, K\}$ . In this paper, states are instantaneous, whereas a regime is a succession of identical states. We denote  $\sigma_t$  the set of possible states at time-step  $t$  with  $\sigma_t = \mathbf{K}$  when  $S_t$  is latent, and  $\sigma_t = \{k\}$  when  $S_t = k$ , that is  $k^{\text{th}}$  state is observed at time-step  $t$ .
- $\mathcal{M}_p(\mathbb{R})$  is the set of square matrices of order  $p$  with real coefficients.
- Symbols in bold represent nonscalar variables (*e.g.*, vectors).

### 3.2 Modelling the state process

Let  $\{(S_t, \sigma_t)\}$  the state process which is supposed to be partially observed. Remind that if  $S_t = k$ , *i.e.*  $k^{\text{th}}$  state has been observed at time-step  $t$ , then  $\sigma_t = \{k\}$ ; otherwise  $\sigma_t = \mathbf{K}$ , *i.e.*  $S_t$  is latent.

Let  $\mathcal{R} = \{k \in \mathbf{K} \mid \exists t \in \mathbb{N}^*, \sigma_t = \{k\}\}$ , the set of states that have been observed at least once. We have  $|\mathcal{R}| \leq K$  where  $K$  is the total number of states. Thus,  $K - |\mathcal{R}|$  states are fully latent and depict the hidden dynamics of the system under study. It has to be underlined that it is difficult (it not sometimes impossible) to associate a physical interpretation to the hidden dynamics. Such an interpretation requires strong knowledge upon the studied system.

In the PHMC-LAR model,  $\{(S_t, \sigma_t)\}$  is modelled by a  $K$ -state PHMC, parametrized by transition probabilities  $a_{i,j} = P(S_t = j \mid S_{t-1} = i)$ ,  $a_{i,j} \in [0, 1]$ ,  $\sum_{j=1}^K a_{i,j} = 1$  and stationary law  $\pi_i = P(S_1 = i)$ ,  $\pi_i \in [0, 1]$ ,  $\sum_{i=1}^K \pi_i = 1$ .

Let  $\boldsymbol{\theta}^{(S)} = ((\pi_i)_{i=1, \dots, K}, (a_{i,j})_{i,j=1, \dots, K})$  denote the set of parameters associated with the PHMC.

### 3.3 Modelling the dynamics under each state

For each state  $k \in \mathbf{K}$ ,  $\{X_t\}$  is supposed to be **stationary** and modelled by a  $p$ -order LAR process defined as follows:

$$X_t \mid X_{t-p}^{t-1}, S_t = k := \phi_{0,k} + \sum_{i=1}^p \phi_{i,k} X_{t-i} + h_k \epsilon_t \quad \text{for } t = 1, \dots, T, \quad (1)$$

with  $p$  the number of past values of  $X_t$  to be used in modelling,  $k$  the state at time-step  $t$ ,  $\boldsymbol{\mu}_k = (\phi_{0,k}, \phi_{1,k}, \dots, \phi_{p,k})$  the intercept and autoregressive parameters associated with  $k^{\text{th}}$  state,  $h_k$  the standard deviation associated with  $k^{\text{th}}$  state and  $\{\epsilon_t\}$  the error terms.

It is important to underline that Eq. 1 is not defined for the  $p$  initial values denoted by  $X_{1-p}^0$ . These initial values are modelled by the initial law  $g_0(x_{1-p}^0; \boldsymbol{\psi})$  parametrized by  $\boldsymbol{\psi}$ . For instance,  $g_0$  can be a multivariate normal distribution  $\mathcal{N}_p(\mathbf{m}, \mathbf{V})$  where  $\mathbf{m} \in \mathbb{R}^p$  is the mean and  $\mathbf{V} \in \mathcal{M}_p(\mathbb{R})$  is the variance-covariance matrix.

The  $\epsilon_t$  terms are independent and identically distributed with zero mean and unit variance. Note that the law of  $\{\epsilon_t\}$  and the conditional distribution  $P(X_t \mid X_{t-p}^{t-1}, S_t = k; \boldsymbol{\mu}_k, h_k)$  belong to the same family. Usually, Gaussian white noises are used. In this case, the conditional distribution is Gaussian too, with mean and variance respectively equal to  $\phi_{0,k} + \sum_{i=1}^p \phi_{i,k} X_{t-i}$  and  $h_k^2$ .

Let  $\boldsymbol{\theta}^{(X,k)} = (\boldsymbol{\mu}_k, h_k)$  the parameters of the LAR( $p$ ) process associated with  $k^{\text{th}}$  state. The law of  $\{X_t\}$  is fully parametrized by  $\boldsymbol{\theta}^{(X)} = (\boldsymbol{\theta}^{(X,k)})_{k=1, \dots, K}$  and  $\boldsymbol{\psi}$ .

To note, as in (Scheffer and Wrobel, 2001) and (Ramasso and Denoeux, 2013), the PHMC-LAR model assumes that the same order  $p$  is shared by all  $|\mathbf{K}|$  LAR processes associated with the states in  $\mathbf{K}$ .

It has also to be highlighted that the state  $S_t = k$  conditioning a LAR process of order  $p$  on  $X_t$  does not impose that the  $p$  lagged values  $X_{t-1}^{t-p}$  be observed under same state  $k$ . That is, the PHMC-LAR model may perfectly switch from regime to regime, and even from state to state, meanwhile keeping memory of values determined by previous regimes or states.

## 4 Learning algorithm

This section is dedicated to the presentation of an instance of the Expectation-Maximization (EM) algorithm, to estimate the PHMC-LAR parameters. As seen in previous subsections, the PHMC component and the LAR components of our model are respectively parametrized by  $\boldsymbol{\theta}^{(S)}$  and  $(\boldsymbol{\theta}^{(X)}, \boldsymbol{\psi})$ . Then, the whole PHMC-LAR model is parametrized by  $(\boldsymbol{\theta}, \boldsymbol{\psi})$  where  $\boldsymbol{\theta} = (\boldsymbol{\theta}^{(S)}, \boldsymbol{\theta}^{(X)})$ . Thus, PHMC-LAR learning consists in estimating  $(\boldsymbol{\theta}, \boldsymbol{\psi})$  from a training dataset.

Thanks to good statistical properties such as asymptotic efficiency, a maximum likelihood estimator (MLE) is considered. However, for models with hidden variables like ours, MLE computation results in an untractable problem. To address this issue, the Expectation-Maximization (EM) algorithm is generally used, in order to approximate a set of parameters that locally maximizes the likelihood function. EM was introduced by [Baum, Petrie, Soules, and Weiss \(1970\)](#) to cope with Hidden Markov Model learning. This version was further extended by [Dempster et al. \(1977\)](#) into the versatile EM algorithm, to handle parameter estimation in a more general framework. EM has also been applied to autoregressive Markov-switching models ([Hamilton, 1990](#)) and PHMC models ([Scheffer and Wrobel, 2001](#); [Ramasso and Denoeux, 2013](#)).

We propose to learn the PHMC-LAR model through a dedicated instance of the EM algorithm. To fix ideas, in subsection 4.1, we first consider the case where the model is trained in a univariate context, that is considering a unique couple of data  $(x_{t=1-p}^T, \sigma_{t=1}^T)$ , with  $x_{t=1-p}^T$  a realization of  $\{X_t\}$  and  $\sigma_t$  the set of possible states at time-step  $t$ . Then, the general multivariate case of  $N$  independent couples of data  $(\mathbf{x}^{(1)}, \Sigma^{(1)}), \dots, (\mathbf{x}^{(N)}, \Sigma^{(N)})$  will be presented in subsection 4.2.

#### 4.1 Particular case: univariate scheme

Let  $\mathbf{x} = x_{1-p}^T$  the observed time series with  $x_{1-p}^0$  the initial values of the autoregressive process. Let  $\Sigma = \sigma_{t=1}^T$ , further simplified into  $\sigma_1^T$ , where  $\sigma_t$  stands for the set of possible states at time-step  $t$ . Let  $(S_1^T, \Sigma)$  the state process (partially observed) of  $\mathbf{x}$  with  $\sigma_t = \mathbf{K}$  if  $S_t$  is hidden, and  $\sigma_t = \{k\}$  if state  $k$  is observed at time-step  $t$ .

MLE is implemented by maximizing the expectation (with respect to the latent variables) of the **complete data likelihood**. Complete data likelihood is further referred to as  $\mathcal{L}^c$ .  $\mathcal{L}^c$  denotes the evidence/likelihood of the training data when latent/hidden variables are supposed to be known.  $\mathcal{L}^c$  writes as follows:

$$\begin{aligned} \mathcal{L}^c(\boldsymbol{\theta}, \boldsymbol{\psi}) &= P(X_{1-p}^T = x_{1-p}^T, S_1^T = s_1^T; \boldsymbol{\theta}, \boldsymbol{\psi}) \\ &= P(X_1^T = x_1^T, S_1^T = s_1^T | X_{1-p}^0 = x_{1-p}^0; \boldsymbol{\theta}) \times P(X_{1-p}^0 = x_{1-p}^0; \boldsymbol{\psi}) \\ &= \mathcal{L}_c^c(\boldsymbol{\theta}) \times g_0(x_{1-p}^0; \boldsymbol{\psi}), \end{aligned} \quad (2)$$

with  $\mathcal{L}_c^c$  the **conditional complete data likelihood** and  $g_0$  the initial law of  $X_t$ .

When the expectation of  $\mathcal{L}^c$  with respect to the partially hidden states is calculated, term  $g_0(x_{1-p}^0; \boldsymbol{\psi})$  in Eq. 2 can be taken out of the expectation since it does not depend on the states:

$$\mathbb{E}_{P(S_1^T | X_{1-p}^T = x_{1-p}^T, \Sigma; \boldsymbol{\theta})}[\mathcal{L}^c(\boldsymbol{\theta}, \boldsymbol{\psi})] = \mathbb{E}_{P(S_1^T | X_{1-p}^T = x_{1-p}^T, \Sigma; \boldsymbol{\theta})}[\mathcal{L}_c^c(\boldsymbol{\theta})] \times g_0(x_{1-p}^0; \boldsymbol{\psi}), \quad (3)$$

where  $P(S_1^T | X_{1-p}^T = x_{1-p}^T, \Sigma; \boldsymbol{\theta})$  is the *posterior probability* of partially hidden states  $(S_1^T, \Sigma)$ .

Then, by considering the logarithmic scale, Eq. 3 can be separately maximized with respect to  $\boldsymbol{\theta}$  and  $\boldsymbol{\psi}$ :

$$\hat{\boldsymbol{\psi}} = \arg \max_{\boldsymbol{\psi}} \ln (g_0(x_{1-p}^0; \boldsymbol{\psi})), \quad (4)$$

$$\hat{\boldsymbol{\theta}} = \arg \max_{\boldsymbol{\theta}} \ln \left( \mathbb{E}_{P(S_1^T | X_{1-p}^T = x_{1-p}^T, \Sigma; \boldsymbol{\theta})}[\mathcal{L}_c^c(\boldsymbol{\theta})] \right). \quad (5)$$

It has to be noted that Eq. 4 is a simple probability observation problem. In contrast, because of the hidden states, maximization with respect to  $\boldsymbol{\theta}$  (Eq. 5) is carried out by an instance of the EM algorithm.

EM is an iterative algorithm that alternates between E(xpectation) step and M(aximization) step. At iteration  $n$ , we obtain:

$$\text{E-step} \quad Q(\boldsymbol{\theta}, \hat{\boldsymbol{\theta}}_{n-1}) = \mathbb{E}_{P(S_1^T | X_{1-p}^T = x_{1-p}^T, \Sigma; \hat{\boldsymbol{\theta}}_{n-1})}[\ln \mathcal{L}_c^c(\boldsymbol{\theta})], \quad (6)$$

$$\text{M-step} \quad \hat{\boldsymbol{\theta}}_n = \arg \max_{\boldsymbol{\theta}} Q(\boldsymbol{\theta}, \hat{\boldsymbol{\theta}}_{n-1}), \quad (7)$$

with  $P(S_1^T | X_{1-p}^T = x_{1-p}^T, \Sigma; \hat{\boldsymbol{\theta}}_{n-1})$  the *posterior probability* of partially hidden states  $(S_1^T, \Sigma)$  at iteration  $n-1$ . The rest of this Subsection details the two EM steps.

#### 4.1.1 Step E of EM

In this step, the quantity  $Q(\boldsymbol{\theta}, \hat{\boldsymbol{\theta}}_{n-1})$  (Eq. 6) is computed. Following the conditional independence graph of the PHMC-LAR model (see Fig. 1b), the conditional complete data likelihood writes:

$$\begin{aligned} \mathcal{L}_c^c(\boldsymbol{\theta}) &= P(X_1^T = x_1^T, S_1^T = s_1^T | X_{1-p}^0; \boldsymbol{\theta}) \\ &= P(S_1 = s_1; \boldsymbol{\theta}^{(S)}) \prod_{t=2}^T P(S_t = s_t | S_{t-1} = s_{t-1}; \boldsymbol{\theta}^{(S)}) \\ &\quad \prod_{t=1}^T P(X_t = x_t | X_{t-p}^{t-1} = x_{t-p}^{t-1}, S_t = s_t; \boldsymbol{\theta}^{(X, s_t)}), \end{aligned} \quad (8)$$

with  $\boldsymbol{\theta}^{(X, k)}$  the parameters of the LAR process associated with  $k^{\text{th}}$  state and  $P(X_t = x_t | X_{t-p}^{t-1} = x_{t-p}^{t-1}, S_t = k; \boldsymbol{\theta}^{(X, k)})$  the conditional law of  $X_t$  within  $k$ .

Notice that the terms in Eq. 8 depend on either a single state  $S_t$  or two consecutive states  $S_t, S_{t-1}$ . In this same equation, products are replaced by sums when considering the logarithm scale. Then  $\ln \mathcal{L}_c^c(\boldsymbol{\theta})$  is substituted in Eq. 6 and the expectation with respect to the posterior probability of state process is developed. After some integrations, we find that  $Q(\boldsymbol{\theta}, \hat{\boldsymbol{\theta}}_{n-1})$  only depends on the following probabilities:

$$\begin{aligned} \xi_t(k, \ell) &= P(S_{t-1} = k, S_t = \ell | X_{1-p}^T = x_{1-p}^T, \Sigma; \hat{\boldsymbol{\theta}}_{n-1}), \\ \text{for } t &= 2, \dots, T, \quad 1 \leq k, \ell \leq K. \end{aligned} \quad (9)$$

$$\begin{aligned} \gamma_t(\ell) &= P(S_t = \ell | X_{1-p}^T = x_{1-p}^T, \Sigma; \hat{\boldsymbol{\theta}}_{n-1}), \\ \text{for } t &= 2, \dots, T, \quad 1 \leq \ell \leq K. \end{aligned} \quad (10)$$

Therefore, the E-step is reduced to computing these probabilities. To this end, we have derived a *backward-forward-backward* procedure as an extension of the forward-backward algorithm, one of the ingredients of the Baum-Welsh algorithm (Dempster et al., 1977). The backward-forward-backward algorithm was initially proposed by Scheffer and Wrobel (2001) for the purpose of PHMC model learning. We have adapted this algorithm to PHMC-LAR models by taking into consideration the autoregressive dynamics. The details about the adapted *backward-forward-backward* algorithm are given in Appendix A.

#### 4.1.2 Step M of EM

At iteration  $n$ , this step consists in maximizing  $Q(\boldsymbol{\theta}, \hat{\boldsymbol{\theta}}_{n-1})$  with respect to parameters  $\boldsymbol{\theta} = (\boldsymbol{\theta}^{(S)}, \boldsymbol{\theta}^{(X)})$ . It is straightforward to show that  $Q(\boldsymbol{\theta}, \hat{\boldsymbol{\theta}}_{n-1})$  can be decomposed as follows:

$$Q(\boldsymbol{\theta}, \hat{\boldsymbol{\theta}}_{n-1}) = Q_S(\boldsymbol{\theta}^{(S)}, \hat{\boldsymbol{\theta}}_{n-1}) + Q_X(\boldsymbol{\theta}^{(X)}, \hat{\boldsymbol{\theta}}_{n-1}),$$

where  $Q_S$  (respectively  $Q_X$ ) only depends on parameters  $\boldsymbol{\theta}_S$  (respectively  $\boldsymbol{\theta}_X$ ). Therefore,  $Q_S$  and  $Q_X$  can be maximized apart:

$$\hat{\boldsymbol{\theta}}_n^{(S)} = \arg \max_{\boldsymbol{\theta}^{(S)}} Q_S(\boldsymbol{\theta}^{(S)}, \hat{\boldsymbol{\theta}}_{n-1}). \quad (11)$$

$$\hat{\boldsymbol{\theta}}_n^{(X)} = \arg \max_{\boldsymbol{\theta}^{(X)}} Q_X(\boldsymbol{\theta}^{(X)}, \hat{\boldsymbol{\theta}}_{n-1}). \quad (12)$$

The analytical expressions of  $Q_S$  and  $Q_X$  are given in Appendix B. Cancelling the first derivative of  $Q_S(\boldsymbol{\theta}^{(S)}, \hat{\boldsymbol{\theta}}_{n-1})$  provides the analytical expression of  $\hat{\boldsymbol{\theta}}_n^{(S)}$ . In contrast, it is not possible to derive the analytical expression for  $\hat{\boldsymbol{\theta}}_n^{(X)}$ . That is why  $Q_X(\boldsymbol{\theta}^{(X)}, \hat{\boldsymbol{\theta}}_{n-1})$  has to be maximized relying on a numerical optimization method (*e.g.*, the quasi-Newton method).

## 4.2 General case: multivariate scheme

We now consider the general case in which PHMC-LAR model is learnt from  $N$  independent couples of data  $(\mathbf{x}^{(1)}, \Sigma^{(1)}), \dots, (\mathbf{x}^{(N)}, \Sigma^{(N)})$ , with  $\mathbf{x}_0^{(1)}, \dots, \mathbf{x}_0^{(N)}$  the associated initial values and  $(\mathbf{S}^{(1)}, \Sigma^{(1)}), \dots, (\mathbf{S}^{(N)}, \Sigma^{(N)})$  the corresponding state processes. It has to be noted that time series  $\mathbf{x}^{(i)}$ 's can have different lengths while their respective initial vectors have a common size ( $\mathbf{x}_0^{(i)} \in \mathbb{R}^p$ , with  $p$  the autoregressive order).

In this case, the MLE estimates of parameters  $(\boldsymbol{\theta}, \boldsymbol{\psi})$  are defined as follows:

$$\hat{\boldsymbol{\psi}} = \arg \max_{\boldsymbol{\psi}} \sum_{i=1}^N \ln \left( g_0(\mathbf{x}_0^{(i)}; \boldsymbol{\psi}) \right), \quad (13)$$

$$\hat{\boldsymbol{\theta}} = \arg \max_{\boldsymbol{\theta}} \ln \left( \mathbb{E}_{P_S} [\mathcal{L}_c^c(\boldsymbol{\theta})] \right), \quad (14)$$

with  $P_S = P(\mathbf{S}^{(1)}, \dots, \mathbf{S}^{(N)} | \mathbf{X}^{(1)} = \mathbf{x}^{(1)}, \dots, \mathbf{X}^{(N)} = \mathbf{x}^{(N)}, \mathbf{X}_0^{(1)} = \mathbf{x}_0^{(1)}, \dots, \mathbf{X}_0^{(N)} = \mathbf{x}_0^{(N)}, \Sigma^{(1)}, \dots, \Sigma^{(N)}; \boldsymbol{\theta})$  the posterior distribution of partially hidden states  $(\mathbf{S}^{(1)}, \Sigma^{(1)}), \dots, (\mathbf{S}^{(N)}, \Sigma^{(N)})$ .

Thus, the conditional complete data likelihood  $\mathcal{L}_c^c(\boldsymbol{\theta})$  defined in Eq. 8 becomes:

$$\begin{aligned} \mathcal{L}_c^c(\boldsymbol{\theta}) &= \prod_{i=1}^N P \left( \mathbf{X}^{(i)} = \mathbf{x}^{(i)}, \mathbf{S}^{(i)} = \mathbf{s}^{(i)} | \mathbf{X}_0^{(i)}; \boldsymbol{\theta} \right) \\ &= \prod_{i=1}^N \left[ P \left( S_1^{(i)} = s_1^{(i)}; \boldsymbol{\theta}^{(S)} \right) \prod_{t=2}^{T_i} P \left( S_t^{(i)} = s_t^{(i)} | S_{t-1}^{(i)} = s_{t-1}^{(i)}; \boldsymbol{\theta}^{(S)} \right) \right. \\ &\quad \left. \times \prod_{t=1}^{T_i} P \left( X_t^{(i)} = x_t^{(i)} | [X^{(i)}]_{t-p}^{t-1} = [x^{(i)}]_{t-p}^{t-1}, S_t^{(i)} = s_t^{(i)}; \boldsymbol{\theta}^{(X, s_t^{(i)})} \right) \right]. \end{aligned} \quad (15)$$

As in Eq. 4, Eq. 13 is a simple probability observation problem. When  $g_0$  is a multivariate normal distribution  $\mathcal{N}_p(\mathbf{m})$ , with mean  $\mathbf{m} \in \mathbb{R}^p$ , variance-covariance matrix  $\mathbf{V} \in \mathcal{M}_p(\mathbb{R})$  and  $\boldsymbol{\psi} = (\mathbf{m}, \mathbf{V})$ , we can show that

$$\hat{\mathbf{m}} = \frac{1}{N} \sum_{i=1}^N \mathbf{x}_0^{(i)}, \quad \hat{\mathbf{V}} = \frac{1}{N} \sum_{i=1}^N (\mathbf{x}_0^{(i)} - \hat{\mathbf{m}}) (\mathbf{x}_0^{(i)} - \hat{\mathbf{m}})', \quad (16)$$

where  $'$  stands for matrix transposition.

Equation 14 is maximized using the instance of EM presented in Subsection 4.1. At each iteration  $n$ , the E-step consists in computing probabilities  $\xi_t^{(i)}$  (Eq. 9) by running the *backward-forward-backward* algorithm presented in Appendix A, on data  $(\mathbf{x}^{(i)}, \Sigma^{(i)})$ . Thus, the expectation  $Q(\boldsymbol{\theta}, \hat{\boldsymbol{\theta}}_{n-1})$  (Eq. 6) can be computed.

Then, in the M-step,  $Q(\boldsymbol{\theta}, \hat{\boldsymbol{\theta}}_{n-1})$  is maximized with respect to  $\boldsymbol{\theta} = (\boldsymbol{\theta}^{(S)}, \boldsymbol{\theta}^{(X)})$  following Eq. 11-12. We obtain the following formula for  $\hat{\boldsymbol{\theta}}_n^{(S)}$ :

$$\hat{a}_{k,l}^{(n)} = \frac{\sum_{i=1}^N \sum_{t=2}^{T_i} \xi_t^{(i)}(k, l)}{\sum_{i=1}^N \sum_{t=1}^{T_i} \gamma_t^{(i)}(k)}, \quad \text{for } 1 \leq k, l \leq K. \quad (17)$$

$$\hat{\pi}_l^{(n)} = \frac{\sum_{i=1}^N \gamma_1^{(i)}(l)}{N}, \quad \text{for } 1 \leq l \leq K, \quad (18)$$

$$\text{with } \gamma_t^{(i)}(s) = P(S_t^{(i)} = s | [X^{(i)}]_{1-p}^{T_i} = x_{1-p}^{T_i}, \Sigma^{(i)}; \hat{\boldsymbol{\theta}}_{n-1}) = \sum_{j=1}^K \xi_2^{(i)}(j, s), \quad (19)$$

for  $t = 2, \dots, T_i$ ,

$$\text{and } \gamma_1^{(i)}(s) = P(S_1^{(i)} = s | [X^{(i)}]_{1-p}^{T_i} = x_{1-p}^{T_i}, \Sigma^{(i)}; \hat{\boldsymbol{\theta}}_{n-1}) = \sum_{j=1}^K \xi_2^{(i)}(s, j). \quad (20)$$

Note that  $\hat{\boldsymbol{\theta}}_n^{(X)}$  is computed through numerical optimization, for instance by using the quasi-Newton method.



Algorithm 1 sums up the instance of EM proposed for PHMC-LAR parameter learning.

---

**Algorithm 1:** EM algorithm for PHMC-LAR model training

---

- 1: **Input:** *data*  $(\mathbf{x}^{(1)}, \Sigma^{(1)}), \dots, (\mathbf{x}^{(N)}, \Sigma^{(N)})$ , precision  $\kappa$ , maximal number of iterations  $max_{iter}$
  - 2: Initialization:  $\hat{\theta}^{(0)}$  randomly chosen
  - 3:  $n \leftarrow 1$
  - 4: **repeat**
  - 5:   E-step
  - 6:     For each couple  $(\mathbf{x}^{(i)}, \Sigma^{(i)})$ ,  $i = 1, \dots, N$
  - 7:     Compute  $\xi_t^{(i)}$  by running the *backward-forward-backward* algorithm on  $(\mathbf{x}^{(i)}, \Sigma^{(i)})$
  - 8:   M-step
  - 9:     M-S : compute  $\hat{\theta}_n^{(S)}$  from Eq. 17-18
  - 10:    M-X : compute  $\hat{\theta}_n^{(X)}$  by numerical optimization of  $Q_X(\theta^{(X)}, \hat{\theta}_{n-1})$
  - 11:     $incr(n)$
  - 12: **until**  $(|\hat{\theta}^{(n)} - \hat{\theta}^{(n-1)}| < \kappa)$  or  $(n > max_{iter})$
  - 13: /\* parameters stay roughly stable between two successive iterations, \*/
  - 14: /\* or the maximum number of iterations is reached \*/
- 

It is well known that the EM algorithm is sensitive to the choice of the starting point  $\hat{\theta}^{(0)}$  as regards the risk of attraction in a local maximum. In practice, several initial values are tested and the model that provides the highest likelihood is chosen. In this work, the initialization procedure presented in Algorithm 2 is used.

---

**Algorithm 2:** EM initialization for PHMC-LAR model training

---

- 1: **Input:**  $L$ , precision  $\kappa$ , maximum number of iterations  $max_{iter}$
  - 2: Let  $\hat{\theta}^{(0,1)}, \dots, \hat{\theta}^{(0,L)}$  initial values randomly chosen.
  - 3: For each  $\hat{\theta}^{(0,j)}$ , EM is run with parameters  $\kappa$  and  $max_{iter}$ .
  - 4: Then,  $\hat{\theta}^{(0)}$  is fixed as the estimated parameters that provide the highest likelihood across the  $L$  restarts.
- 

## 5 Hidden state inference

In HMM modelling, after a model is learnt, inference consists in finding the state sequence that maximizes the likelihood of a given observed sequence. This is equivalent to solve a *Maximum A Posteriori* (MAP) problem. The Greedy search method that enumerates all combinations of states requires  $\mathcal{O}(K^T)$  operations, where  $K$  is the number of states and  $T$  is the sequence length. The **Viterbi algorithm** designed by Forney (1973) computes the optimal state sequence in  $\mathcal{O}(TK^2)$  operations.

In this section, we propose a variant of the Viterbi algorithm that takes into account the observed states of the PHMC-LAR model. Thus, the hidden states are inferred given the observed states and the given observation sequence.

Let  $\hat{\theta}$  the MLE parameter estimates of the PHMC-LAR model trained on a given dataset. Let  $\mathbf{x} = x_1^T$  an observed time series and  $\mathbf{x}_0 = x_{1-p}^0$  the corresponding initial values. Let  $\Sigma = \sigma_{t=1}^T$  the possible states at each time-step with  $\sigma_t = \{k\}$  if  $k^{th}$  regime is observed at time-step  $t$ , and  $\sigma_t = \mathbf{K}$  if the state process is latent at that time-step. Let  $(\mathbf{S}, \Sigma)$  the partially hidden state process associated with this time series.

We search the optimal state sequence  $\mathbf{z}^* = (z_1^*, \dots, z_T^*)$  that maximizes the posterior probability  $P(\mathbf{S} = \mathbf{z} | \mathbf{X} = \mathbf{x}, \mathbf{X}_0 = \mathbf{x}_0, \Sigma; \hat{\theta})$ . Thanks to Bayes' rule, maximizing this posterior probability is equivalent to maximizing the joint probability  $P(\mathbf{S} = \mathbf{z}, \mathbf{X} = \mathbf{x} | \mathbf{X}_0 = \mathbf{x}_0, \Sigma; \hat{\theta})$ :

$$P(\mathbf{S} = \mathbf{z} | \mathbf{X} = \mathbf{x}, \mathbf{X}_0 = \mathbf{x}_0; \hat{\theta}^{(X)}) = \frac{P(\mathbf{S} = \mathbf{z}, \mathbf{X} = \mathbf{x} | \mathbf{X}_0 = \mathbf{x}_0, \Sigma; \hat{\theta})}{P(\mathbf{X} = \mathbf{x} | \mathbf{X}_0 = \mathbf{x}_0, \Sigma; \hat{\theta}^{(S)})}. \quad (21)$$

$$\mathbf{z}^* = \arg \max_{\mathbf{z} \in \mathbf{K}^T} P(\mathbf{S} = \mathbf{z}, \mathbf{X} = \mathbf{x} | \mathbf{X}_0 = \mathbf{x}_0, \Sigma; \hat{\theta}), \quad (22)$$

where  $\mathbf{K} = \{1, 2, \dots, K\}$  is the set of possible states.

Note that the probability of a given state sequence is null if there is at least a time-step  $t$  such that  $z_t \notin \sigma_t$ , that is if state  $z_t$  is not allowed at time-step  $t$ . A consequence is that  $\mathbf{z}^*$  must coincide with the observed states if there are any.

Following the dynamic programming paradigm, the Viterbi algorithm makes it possible to retrieve  $\mathbf{z}^*$  by splitting the initial problem into subproblems and solving this set of smaller problems. Let  $\delta_t(\ell; \hat{\boldsymbol{\theta}})$  the maximal probability of subsequence  $(z_1, \dots, z_t = \ell)$  that ends within regime  $\ell$ :

$$\delta_t(\ell; \hat{\boldsymbol{\theta}}) = \max_{z_1, \dots, z_{t-1} \in \mathbf{K}^{t-1}} P(X_1^t = x_1^t, S_1^{t-1} = z_1^{t-1}, S_t = \ell | \mathbf{X}_0 = \mathbf{x}_0, \sigma_1^t; \hat{\boldsymbol{\theta}}), \quad (23)$$

for  $t = 1, 2, \dots, T$ .

These probabilities are iteratively computed as follows:

At first time-step,

$$\delta_1(\ell; \hat{\boldsymbol{\theta}}) = P(X_1 = x_1 | \mathbf{X}_0 = \mathbf{x}_0, S_1 = \ell; \boldsymbol{\theta}^{(X, \ell)}) \times P(S_1 = \ell | \sigma_1; \hat{\boldsymbol{\theta}}^{(S)}) \quad (24)$$

where

$$P(S_1 = \ell | \sigma_1; \hat{\boldsymbol{\theta}}^{(S)}) = \begin{cases} \hat{\pi}_\ell & \text{if } \ell \in \sigma_1 \\ 0 & \text{otherwise.} \end{cases}$$

For  $t = 2, \dots, T$  we have

$$\delta_t(\ell; \hat{\boldsymbol{\theta}}) = \max_k \left[ \delta_{t-1}(k; \hat{\boldsymbol{\theta}}) P(S_t = \ell | S_{t-1} = k, \sigma_t; \hat{\boldsymbol{\theta}}^{(S)}) \right] \times P(X_t = x_t | X_1^{t-1} = x_1^{t-1}, \mathbf{X}_0 = \mathbf{x}_0, S_t = \ell; \boldsymbol{\theta}^{(X, \ell)}), \quad (25)$$

with

$$P(S_t = \ell | S_{t-1} = k, \sigma_t; \hat{\boldsymbol{\theta}}^{(S)}) = \begin{cases} \hat{a}_{k, \ell} & \text{if } \ell \in \sigma_t \text{ and } k \in \sigma_{t-1} \\ 0 & \text{otherwise.} \end{cases}$$

Since the maximal probability of the complete state sequence, that is the maximum for the probability expressed in Eq. 21, also writes:

$$P^* = \max_{\ell} \delta_T(\ell; \hat{\boldsymbol{\theta}}), \quad (26)$$

the optimal sequence  $\mathbf{z}^*$ , defined in Eq. 22 is retrieved by backtracking as follows:

$$z_t^* = \arg \max_{\ell} \begin{cases} \delta_T(\ell; \hat{\boldsymbol{\theta}}) & \text{for } t = T \\ \delta_t(\ell; \hat{\boldsymbol{\theta}}) \times \hat{a}_{\ell, z_{t+1}^*} & \text{for } t = T-1, \dots, 1. \end{cases} \quad (27)$$

## 6 Forecasting

Forecasting for a time series consists in predicting future values based on past values. Let us consider a PHMC-LAR model trained on a sequence observed up to time-step  $T$ , and  $\hat{\boldsymbol{\theta}}$  the corresponding parameters. Let  $\sigma_{T+1}, \dots, \sigma_{T+h}$  the set of possible states from time-step  $T+1$  to time-step  $T+h$ .

The optimal prediction of  $X_{T+h}$  (with respect to mean squared error) is the conditional mean  $\mathbb{E}[X_{T+h} | X_{1-p}^T = x_{1-p}^T, \sigma_{T+1}^{T+h}; \hat{\boldsymbol{\theta}}]$ , which writes as follows:

$$\begin{aligned} \hat{X}_{T+h} &= \sum_{k=1}^K P(S_{T+h} = k | X_{1-p}^T = x_{1-p}^T, \sigma_{T+1}^{T+h}; \hat{\boldsymbol{\theta}}) \\ &\quad \mathbb{E}[X_{T+h} | X_{T+h-p}^{T+h-1} = x_{T+h-p}^{T+h-1}, S_{T+h} = k; \hat{\boldsymbol{\theta}}] \\ &= \sum_{k=1}^K P(S_{T+h} = k | X_{1-p}^T = x_{1-p}^T, \sigma_{T+1}^{T+h}; \hat{\boldsymbol{\theta}}) \left( \mathbf{y}_{T+h} \hat{\boldsymbol{\mu}}_k' \right), \end{aligned} \quad (28)$$

with  $\mathbf{y}_{T+h} = (1, x_{T+h-1}, \dots, x_{T+h-p})$ ,  $\hat{\boldsymbol{\mu}}_k = (\phi_{0,k}, \phi_{1,k}, \dots, \phi_{p,k})$  the intercept and autoregressive parameters associated with  $k^{\text{th}}$  state, and  $'$  denoting matrix transposition.

Equation 28 depends on **smoothed probabilities**  $\bar{\gamma}(i, s) = P(S_{T+i} = s | X_{1-p}^T = x_{1-p}^T, \sigma_{T+1}^{T+i}; \hat{\boldsymbol{\theta}})$ , which are recursively computed as follows:

$$\begin{cases} \bar{\gamma}(0, s) = P(S_T = s | X_{1-p}^T = x_{1-p}^T; \hat{\boldsymbol{\theta}}) = \gamma_T(s), \\ \bar{\gamma}(i, s) = \sum_{\ell=1}^K \hat{a}_{\ell,s} \bar{\gamma}(i-1, \ell) & \text{if } \sigma_{T+i} = \mathbf{K}, \\ \bar{\gamma}(i, s) = 1 & \text{if } \sigma_{T+i} = \{\ell\} \text{ and } s = \ell, \\ \bar{\gamma}(i, s) = 0 & \text{if } \sigma_{T+i} = \{\ell\} \text{ and } s \neq \ell, \end{cases} \quad (29)$$

for  $i = 1, \dots, h$ ,  $s \in \mathbf{K}$  and  $\gamma_T(l)$  defined in Eq. 19.

From Eq. 28 and 29, we can notice that if state  $s$  is observed at time-step  $T+h$  (*i.e.*  $\sigma_{T+h} = \{s\}$ ), then prediction  $\hat{X}_{T+h}$  equals the conditional mean of the LAR process associated with this state (since  $\bar{\gamma}(h, k) = 0$  for  $k \notin \sigma_{T+h}$ ). In contrast, if state process is latent at time-step  $T+h$  (*i.e.*,  $\sigma_{T+h} = \mathbf{K}$ ),  $\hat{X}_{T+h}$  is computed as the weighted sum of the conditional means of all states, with probabilities  $\bar{\gamma}(h, k)$  as weights.

Note that for  $h = 1$ , the past values of the time series required in Eq. 28 are known. In contrast, for  $h > 1$ , the intermediate predictions  $\hat{X}_{T+1}, \dots, \hat{X}_{T+h-1}$  are used in order to feed the autoregressive dynamics of the PHMC-LAR framework.

## 7 Experiments

The aim of this section is two-fold: (i) assess the ability of PHMC-LAR model to infer the hidden states, (ii) evaluate prediction accuracy. These evaluations were achieved on simulated data, following two experimental settings. On the one hand, we varied the percentage of observed states in training set, to evaluate its influence on hidden state recovery and prediction accuracy. On the other hand, we simulated unreliable observed states in training set, and evaluated the influence of uncertain labelling on hidden state inference and prediction accuracy.

This section starts with the description of the protocol used to simulate data in both experimental settings. Then, the section focuses on implementation aspects. We next present and discuss the results obtained in both experimental settings.

### 7.1 Simulated datasets

This subsection first focuses on the model used to generate data. Then we describe the precursor sets used to further generate the test-set and the training datasets.

#### 7.1.1 Generative model

These experiments were achieved on simulated data from a 4-state PHMC-LAR(2) model whose transition matrix and initial probabilities are:

$$A = \begin{pmatrix} 0.5 & 0.2 & 0.1 & 0.2 \\ 0.2 & 0.5 & 0.2 & 0.1 \\ 0.1 & 0.2 & 0.5 & 0.2 \\ 0.2 & 0.1 & 0.2 & 0.5 \end{pmatrix}, \quad \pi = (0.25, 0.25, 0.25, 0.25). \quad (30)$$

Within each state  $k \in \{1, 2, 3, 4\}$ , the autoregressive dynamics is a LAR(2) process defined by parameters  $\boldsymbol{\theta}^{(X,k)} = (\phi_{0,k}, \phi_{1,k}, \phi_{2,k}, h_k)$ :

$$\begin{aligned} \boldsymbol{\theta}^{(X,1)} &= (2, 0.5, 0.75, 0.2), & \boldsymbol{\theta}^{(X,2)} &= (-2, -0.5, 0.75, 0.5), \\ \boldsymbol{\theta}^{(X,3)} &= (4, 0.5, -0.75, 0.7), & \boldsymbol{\theta}^{(X,4)} &= (-4, -0.5, -0.75, 0.9). \end{aligned} \quad (31)$$

In the LAR(2) process associated with state  $k$ , stationarity is guaranteed by setting the following constraints:  $\phi_{i,k} < 1$ ,  $i \in \{1, 2\}$ .

Finally, the initial law  $g_0$  is a bivariate Gaussian distribution

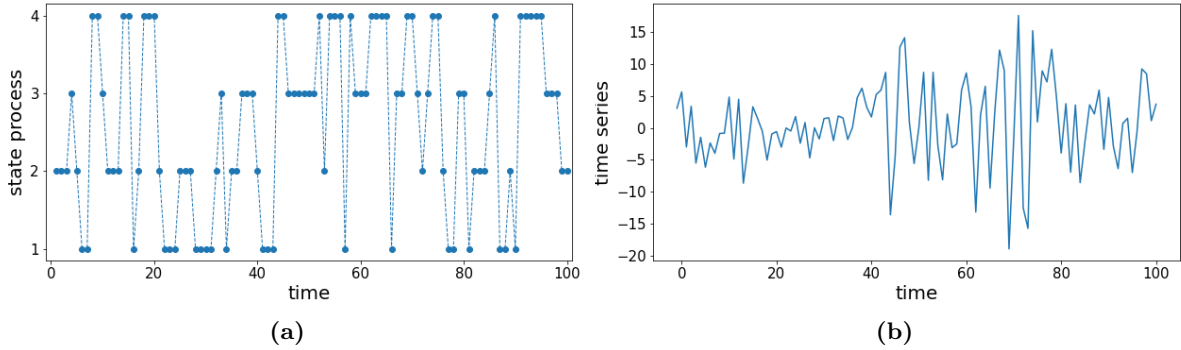


**Figure 2** A simulation from the PHMC-LAR(2) model defined by Eq. 30-32: (a) state process, (b) the corresponding time series

$$g_0 = \mathcal{N}_2 \left( (3, 5), \begin{pmatrix} 1 & 0.1 \\ 0.1 & 1 \end{pmatrix} \right). \quad (32)$$

Figure 2 shows an example of state process (Fig. 2a) and corresponding time series (Fig. 2b) that were simulated from the previously defined PHMC-LAR(2).

### 7.1.2 Precursor sets for the test-set and training datasets

The training and test sets are common to both experimental settings (influence of the percentage of observed labels, influence of labelling error).

**Inference** The precursor set  $\mathcal{P}_{infer.test}$  of the test-set is composed of  $M = 100$  fully labelled observation sequences of length  $\ell = 1000$ . These sequences were generated from the PHMC-LAR(2) model described in Eq. 30-32. A protocol repeated for each  $N \in \{1, 10, 100\}$  produced a precursor set  $\mathcal{P}_{N.infer.train}$  consisting of  $N$  fully labelled observation sequences of length  $T = 100$ . The generative model in Eq. 30-32 was used for this purpose.

**Forecasting** In this case, training sets are each reduced to a single sequence. In each such sequence, the sequence’s prefix of size  $T = 100$  is used for model training, whereas the subsequence  $T + 1, \dots, T + 10$  is used for testing prediction accuracy. The sequences of the unique precursor set denoted  $\mathcal{P}_{N=1.forecast.train.test}$  are generated using Eq. 30-32.

## 7.2 Implementation

Our experiments required intensive computing resources from a Tier 2 data centre (Intel 2630v4,  $2 \times 10$  cores 2.2 Ghz,  $20 \times 6$  GB). We exploited data-driven parallelization to replicate our experiments on various training sets. On the other hand, code parallelization allowed us to process multiple sequences simultaneously in the step E of the EM algorithm. The software programs dedicated to model training, hidden state inference and forecasting were written in Python 3.6.9. We used the NumPy and SciPy Python libraries.

The models were learnt through the EM algorithm with precision  $\kappa = 10^{-6}$  and initialization procedure parameters  $(L, N_{iter}) = (5, 10)$ .

### 7.3 Influence of the percentage of observed states

To analyze the impact of observed states, we varied the percentage  $P$  of labelled observations (equivalently the percentage of observed states) in the training sets.  $P$  was varied from 0% (fully unsupervised case) to 100% (fully supervised case), with steps of 10%. The aim is to evaluate the performance of intermediate cases for different sizes of the training datasets.

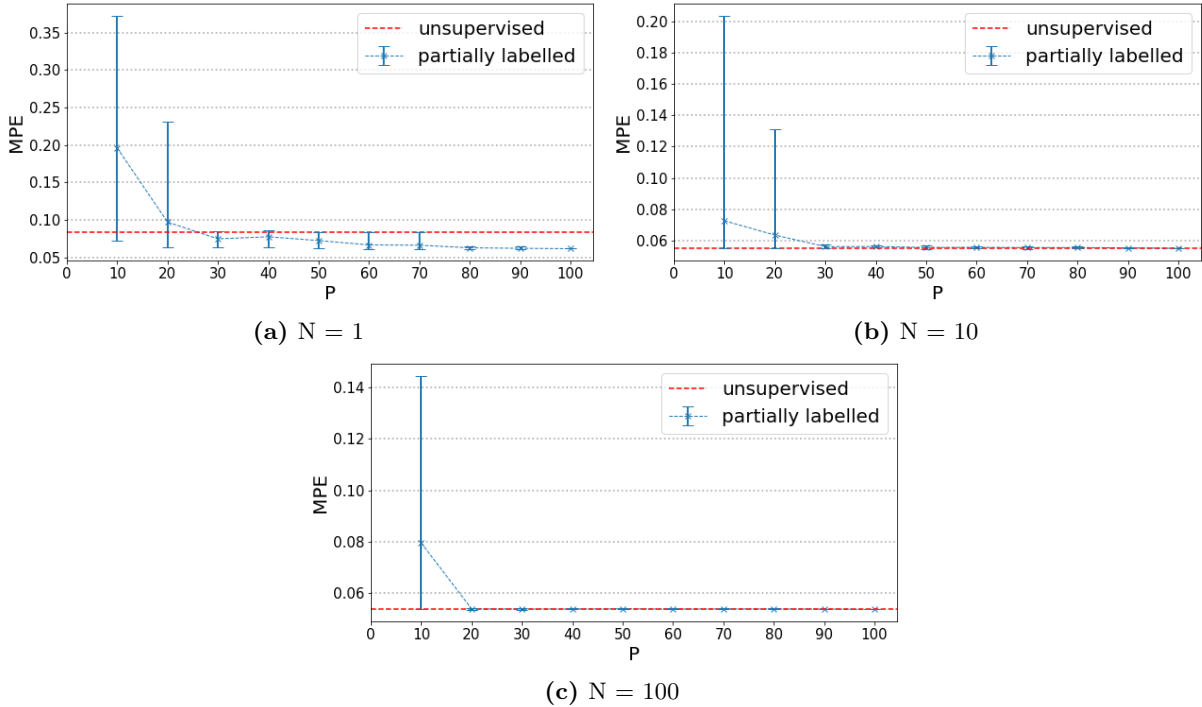


**Figure 3** 95% confidence interval for mean percentage error (MPE) of hidden state inference, as a function of the percentage  $P$  of labelled observations. Models were trained on datasets of  $N$  sequences of length 100, for each of 15 replicates differing by the  $P\%$  labelled observations. For each model, inference was performed for a test-set of 100 unlabelled sequences of size 1000. The 95% confidence interval of the MPE score was computed from the 15 replicates. The dash (red) line indicates the MPE score obtained for the unsupervised learning case ( $P = 0\%$ ). Mind the differences in scales between the three subfigures.

### 7.3.1 Hidden state inference

The test-set  $\mathcal{S}_{infer\_test}$  was generated by unlabelling all states from the precursor set  $\mathcal{P}_{infer\_test}$  described in Subsection 7.1.2 ( $M = 100$  fully observed sequences of length  $\ell = 1000$ ).

To generate the training sets, the following protocol was repeated for each  $N \in \{1, 10, 100\}$  and for each percentage  $P$ : (i) considering the appropriate precursor set  $\mathcal{P}_{N\_infer\_train}$  ( $N$  fully observed sequences of length  $T = 100$ ) depicted in Subsection 7.1.2, only a proportion of  $P$  observations was kept labelled while the rest was unlabelled; (ii) this process was repeated 15 times, each time varying which observations are kept labelled. Thus were produced 15 training datasets  $\mathcal{S}_{N\_P\_infer\_train\_1}, \dots, \mathcal{S}_{N\_P\_infer\_train\_15}$ .

The PHMC-LAR(2) model with 4 states was trained on each training set  $\mathcal{S}_{N,P,infer\_train,i}$ ,  $i = 1, \dots, 15$ . For each trained model, state inference was achieved for the  $M$  fully hidden sequences of test-set  $\mathcal{S}_{infer\_test}$ , which yielded  $M$  sequences of predicted labels. Inference performance was evaluated by comparing the true state sequences with the inferred ones, using the **Mean Percentage Error** (MPE) score defined as follows:

$$\text{MPE} = \frac{1}{M} \sum_{i=1}^M \left[ \frac{1}{\ell} \sum_{j=1}^{\ell} \mathbf{1}_{s_j \neq \hat{s}_j} \right], \quad (33)$$

where  $s_j$ 's and  $\hat{s}_j$ 's are respectively observed and inferred states. The MPE score varies between 0 and 1. The lower the value of the MPE score, the higher the inference performance.

Figure 3 displays 95% confidence interval for the MPE score as a function of  $P$ . As expected, the results show that inference ability increases with the number of training sequences denoted by  $N$ . Note that when the proportion of labelled observations is less than some threshold ( $P = 30\%$  for  $N = 1, 10$  and  $P = 20\%$  for  $N = 100$ ), inference performance is greatly impacted by the distribution of observed states since we obtain very large confidence intervals for the MPE score.

For  $N = 1$ , the use of labelled observations makes it possible to outperform the fully unsupervised case ( $P = 0\%$ ) (which translates into small MPE scores) when at least 30% of observations are labelled (see Fig. 3a). In contrast,

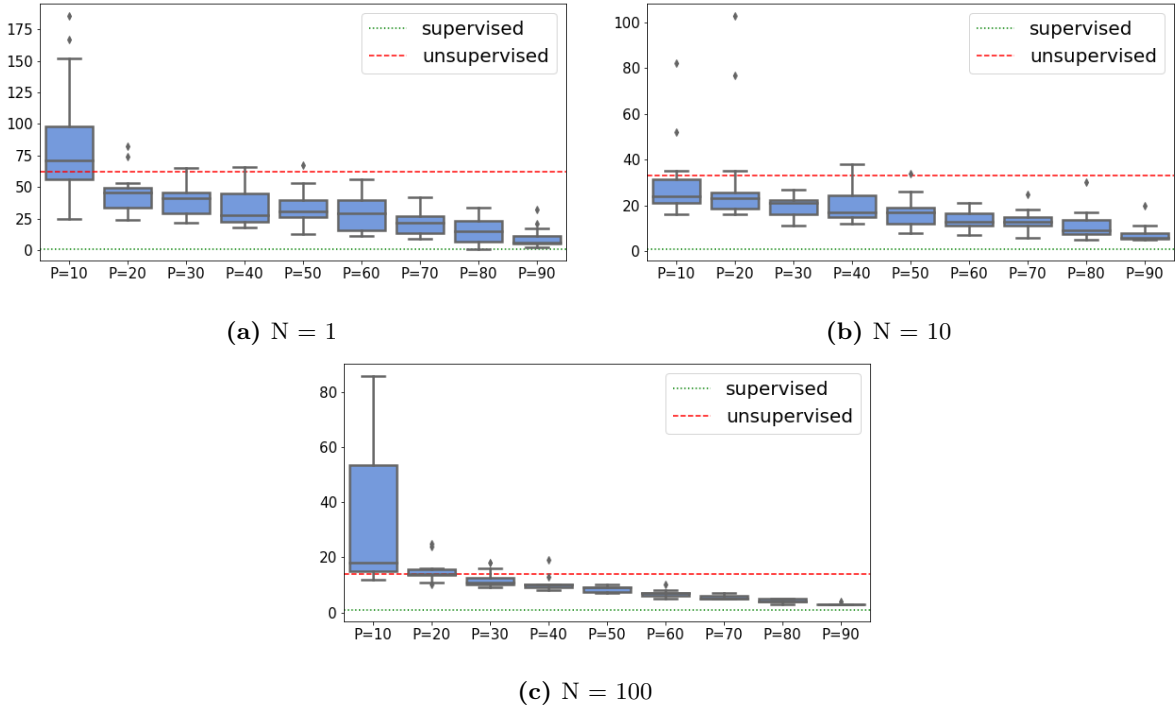


**Figure 4** Number of EM iterations before convergence as a function of the percentage  $P$  of labelled observations. For the description of the experimental protocol, see caption of Fig.3. The distribution of the number of EM iterations is studied across 15 replicates. Dash (red) line and dot (green) line indicate the number of iterations for unsupervised and supervised learning cases respectively. Mind the differences in scales between the three subfigures.

for  $N = 10, 100$ , from some threshold value of  $P$  (respectively 30% and 20%), the use of larger proportions of labelled observations sustains inference performances equal to that of the fully unsupervised case (see Fig. 3b and 3c). Importantly, the results show that using large proportions of labelled observations considerably speeds up model training by decreasing the number of iterations of the EM algorithm (see Fig. 4), and allows to better characterize the training data (which is reflected by a greater likelihood, see Fig. 5). Ramasso and Denoeux (2013) had already underlined the beneficial impact of partial knowledge integration on EM convergence in HPMCs. Our work confirms this advantage in the PHMC-LAR model, with a good preservation of inference performance.

In order to evaluate the influence of observed states in recognition phase, we considered the case  $P = 10\%$  which previously obtained the lowest inference performance. This time, we also kept labelled a proportion  $Q$  of observations within the test-set  $\mathcal{S}_{infer.test}$ . We assessed the inference performances for the models trained on  $\mathcal{S}_{N,P=10\%,infer.train,i}$ ,  $i = 1, \dots, 15$ . Figure 6 presents MPEs as a function of  $Q$  for  $N = 1, 10$  and 100. We observe that inference performances are improved by the presence of observed states. More precisely, for  $Q$  taking its values in 25%, 50% and 75%, respectively, MPE decreases by: (i) 19%, 42% and 69% for  $N = 1$  (Fig. 6a); (ii) 27%, 52% and 77% for  $N = 10$  (Fig. 6b); and (iii) 27%, 53% and 77% for  $N = 100$ . (Fig. 6c). These results show the ability of our variant of the Viterbi algorithm to infer partially-labelled sequences.

### 7.3.2 Forecasting

In this experiment, we consider models trained on a single sequence. This case corresponds to many real-world situations in which a unique time series is available (*e.g.*, the evolution of air pollution at some geographical location). Using the precursor set  $\mathcal{P}_{N=1-forecast.train.test}$  described in Subsection 7.1.2, we generated datasets  $\mathcal{S}_{N=1-forecast.train.test,i}$ ,  $i = 1, \dots, 15$  each composed of a single sequence of size 110. Again, the 15 replicates differed by the  $P\%$  labelled observations. In these sets, the sequence prefixes of length  $T = 100$  were used to train the models. *Out-of-sample* forecasting was carried out at horizons  $T+h$ ,  $h = 1, \dots, 10$ , which means that prediction accuracy was assessed using subsequences  $T+1, \dots, T+h$ . To note, the  $P\%$  labelled observations were distributed in the sequence prefixes of length  $T$ .

Two experimental schemes were considered. First, the states at forecast horizons were supposed to be latent; that is, all states were unlabelled from  $T+1$  to  $T+h$ ,  $h = 1, \dots, 10$ . Then, we performed the prediction evaluation when

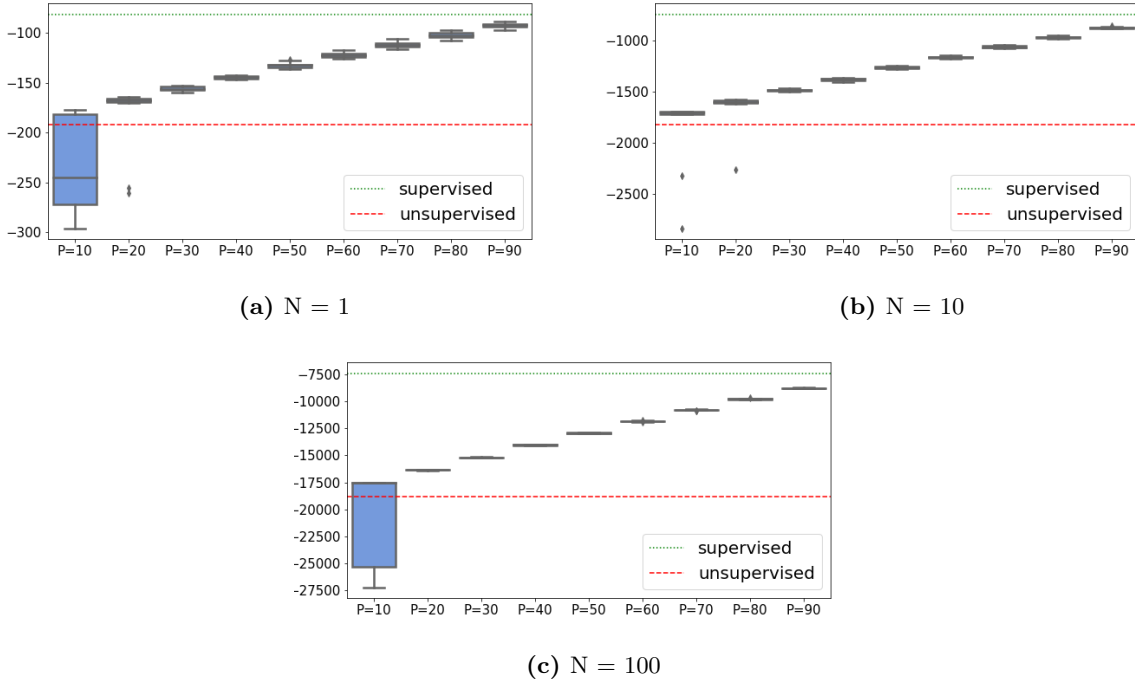


**Figure 5** Log-likelihood as a function of the percentage  $P$  of labelled observations. For the description of the experimental protocol, see caption of Fig.3. The distribution of the log-likelihood is studied across 15 replicates. Dash (red) line and dot (green) line indicate the log-likelihoods for unsupervised and supervised learning cases respectively. Mind the differences in scales between the three subfigures.

states are observed at forecast horizons. The latter situation corresponds to performing the prediction conditional on some assumption on the regime. For instance, in econometrics, assuming we know which phase will be on (growth phase *versus* recession) might improve the forecasting performance of the Gross National Product (GNP). In this case, all states were kept labelled from  $T + 1$  to  $T + h$ ,  $h = 1, \dots, 10$ .

Prediction performance is estimated by the **Root Mean Square Error** (RMSE) defined as follows:

$$\text{RMSE}_h = \sqrt{\frac{1}{N_{rep}} \sum_{i=1}^{N_{rep}} (X_{T+h}^{(i)} - \hat{X}_{T+h}^{(i)})^2}, \quad (34)$$

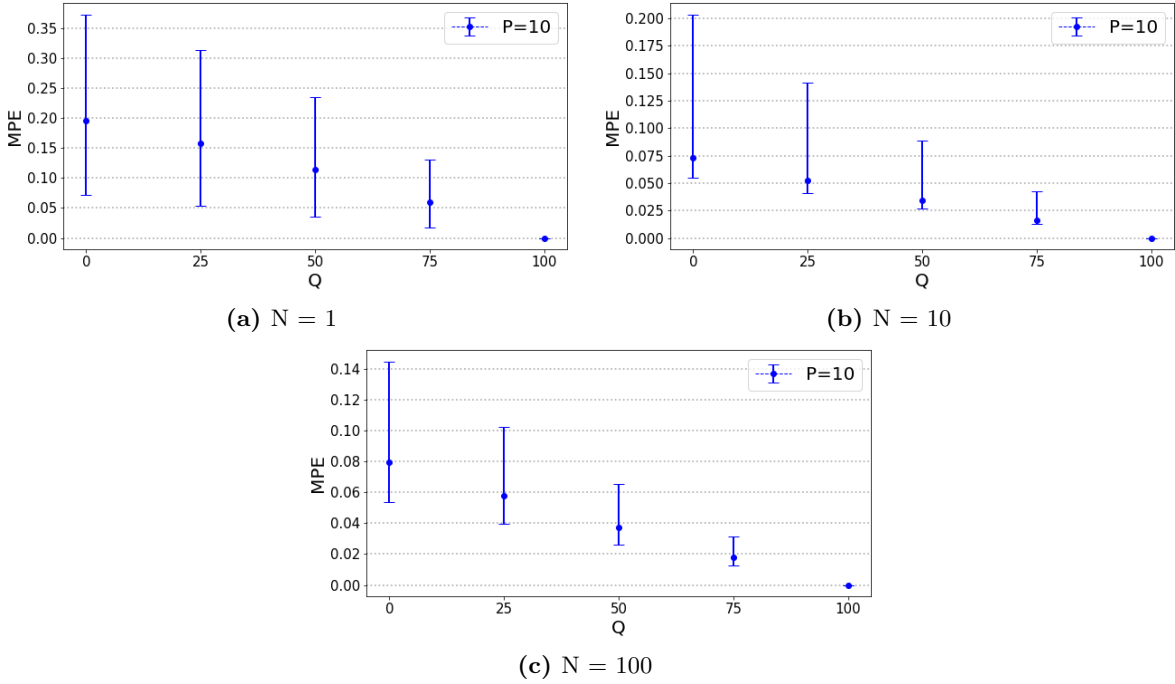
where  $h$  is the forecast horizon and  $N_{rep} = 15$  is the number of replicates. Accurate predictions are characterized by low RMSEs.

Table 1 presents the RMSEs obtained when the states at forecast horizons are supposed to be latent. Fig. 7a presents the mean, median and maximum of RMSEs, computed over all forecast horizons, as a function of  $P$ , the percentage of labelled observations in the training sets. Table 1 and Fig. 7a show that as from some low  $P$  threshold (10% or 20%), the prediction performance remains nearby constant across proportions.

In addition, Table 1 also highlights that the ability to predict depends on the forecast horizon under consideration. At any given labelling percentage  $P$ , high RMSE scores (*i.e.*, around 7) alternate with low scores (around 1) across horizons. The nonmonotonic error trend across horizons was observed empirically for MS-AR models and threshold autoregressive models when they are applied to US GNP time series (Clements and Krolzig, 1998).

Finally, our experiments show that PHMC-LAR model's ability to better characterize the training data in presence of large proportions of labelled observations (characterized by greater likelihood, see Fig. 5a) does not translate into an improved forecast performance.

When states are known at forecast horizons, RMSEs (presented in Table 2) are reduced by 44% on average. Moreover, Fig. 7b shows that above percentage  $P = 30\%$ , prediction performances are slightly greater than that of the unsupervised case ( $P = 0\%$ ). Note that as in the case when the states are unknown at forecast horizons, the prediction ability depends on the forecast horizon. Again, for a given  $P$ , the RMSE score does not systematically increase with forecast horizon  $h$ , although previously predicted values are used as inputs when predicting at next horizons.



**Figure 6** 95% confidence interval for mean percentage error (MPE) of hidden state inference, as a function of the percentage  $Q$  of labelled observations within test-set, with  $P = 10\%$  labelled observations in the training sets. Models were trained on datasets of  $N$  sequences of length 100 in which  $P = 10\%$  of observations have been labelled. Fifteen replicates differing by the  $P = 10\%$  labelled observations were considered. For each model, inference was performed for a test-set of 100 partially labelled ( $Q\%$ ) sequences of size 1000. **The 95% confidence interval of the MPE score was computed from the 15 replicates.** Mind the differences in scales between the three subfigures.

$P \backslash h_1$	2	3	4	5	6	7	8	9	10	
0	1.860	<b>6.680</b>	1.830	3.165	4.167	2.540	1.133	7.938	7.854	2.465
10	2.035	8.273	1.829	<b>2.909</b>	4.477	2.851	<b>0.957</b>	<b>7.667</b>	<b>7.583</b>	<b>2.224</b>
20	1.934	7.612	<b>1.337</b>	3.161	4.110	2.482	1.189	7.991	7.907	2.518
30	1.323	7.450	1.373	3.168	<b>4.093</b>	<b>2.469</b>	1.201	8.005	7.921	2.532
40	1.293	7.496	1.392	3.158	4.103	2.480	1.191	7.994	7.911	2.521
50	1.308	7.525	1.402	3.135	4.122	2.496	1.174	7.978	7.894	2.505
60	1.394	7.502	1.424	3.115	4.134	2.508	1.162	7.965	7.882	2.493
70	1.363	7.560	1.431	3.094	4.155	2.527	1.142	7.946	7.862	2.473
80	1.306	7.502	1.395	3.129	4.116	2.489	1.179	7.984	7.900	2.511
90	1.294	7.569	1.444	3.088	4.155	2.526	1.142	7.947	7.863	2.473
100	<b>1.267</b>	7.613	1.447	3.076	4.164	2.535	1.132	7.937	7.854	2.464

**Table 1** Root mean square error (RMSE) of prediction at horizon  $h$  for different values of  $P$ , when the states are unknown throughout forecast horizons.  $P$  is the percentage of labelled observations within the training datasets. The forecast horizons are time-steps  $T + 1$  to  $T + h$ ,  $T = 100$ . For a given value of  $P$ , models were each trained on a unique sequence: the sequence’s prefix of length  $T = 100$  was used for training, for each of 15 replicates differing by the  $P\%$  labelled observations distributed in the prefix. Then, out-of-sample forecasting was carried out at time-steps  $T + 1, \dots, T + 10$ , for the same sequence. The figures in bold highlight the minimum RMSE obtained across all labelling percentages ( $P$ ), at each horizon ( $h$ ) considered

## 7.4 Influence of labelling error

In this experiment, the influence of labelling error is evaluated. To simulate unreliable labels, we proceeded as follows.

At each time-step  $t$ , an error probability  $p_t$  was drawn randomly from a beta distribution with mean  $\rho$  and variance 0.2. With probability  $p_t$ , the observed state  $s_t$  was replaced by a random state uniformly chosen from



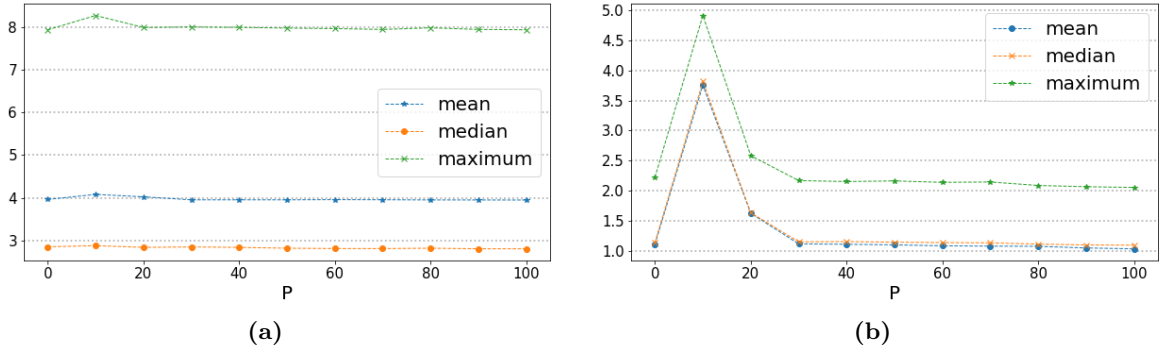


**Figure 7** Mean, median and maximum root mean square error (RMSE) of prediction at horizon  $h$  as a function of  $P$ , the percentage of labelled observations in the training datasets. States at forecast time-steps  $T + h$ ,  $h = 1, \dots, 10$  are (a) hidden, (b) known. Models were trained on a single sequence, for each of 15 replicates differing by the  $P\%$  labelled observations. Model training was performed on subsequences of length 100, whereas prediction was achieved for the 10 subsequent time-steps. For each value of  $P$ , the statistics provided were computed across the 15 replicates and all horizons.

$P \backslash h_1$	1	2	3	4	5	6	7	8	9	10
0	0.083	0.325	0.870	1.577	1.509	1.171	2.220	1.216	<b>0.996</b>	<b>1.104</b>
10	3.730	1.791	2.936	3.593	4.914	4.153	4.060	4.873	3.603	3.902
20	1.831	0.510	1.806	1.939	2.171	1.250	2.581	1.438	1.239	1.458
30	0.083	<b>0.321</b>	0.854	1.542	1.477	1.158	2.167	1.137	1.109	1.289
40	0.070	0.325	0.841	1.532	1.460	1.150	2.151	1.154	1.084	1.301
50	0.065	0.324	0.832	1.540	1.459	1.154	2.161	1.130	1.078	1.229
60	0.063	0.329	0.829	1.524	1.443	1.145	2.137	1.125	1.039	1.181
70	0.057	0.329	0.810	1.531	1.431	1.143	2.143	1.118	1.036	1.263
80	0.036	0.327	0.810	1.490	1.411	1.134	2.086	1.086	1.072	1.276
90	0.036	0.325	0.788	1.479	1.386	1.124	2.065	1.067	1.023	1.161
100	<b>0.001</b>	0.326	<b>0.760</b>	<b>1.473</b>	<b>1.368</b>	<b>1.121</b>	<b>2.053</b>	<b>1.065</b>	1.002	1.133

**Table 2** Root mean square error (RMSE) of prediction at horizon  $h$  for different values of  $P$ , when the states are known throughout forecast horizons.  $P$  is the percentage of labelled observations within the training datasets. The forecast horizons are time-steps  $T + 1$  to  $T + h$ ,  $T = 100$ . For the description of the experimental protocol, see caption of Table 1. The states are known from  $T + 1$  to  $T + 10$  time-steps. The figures in bold highlight the minimum RMSE obtained across all labelling percentages ( $P$ ), at each horizon ( $h$ ) considered

$\{1, 2, 3, 4\} \setminus \{s_t\}$ . So, the unreliable labels  $\tilde{s}_t$  were defined as follows:

$$\begin{aligned}
 p_t &\sim \beta(0.2, \rho) \\
 \tilde{s}_t &= \begin{cases} s_t & \text{with probability } 1 - p_t \\ \mathcal{U}(\{1, 2, 3, 4\} \setminus \{s_t\}) & \text{with probability } p_t \end{cases} \quad (35)
 \end{aligned}$$

where  $\mathcal{U}$  is the discrete-valued uniform distribution. Thus, on average a proportion  $\rho$  of observations is assigned wrong labels.

#### 7.4.1 Inference of hidden states

To assess inference performance in presence of labelling errors, we relied on the test-set  $\mathcal{S}_{infer.test}$  described in Subsection 7.3 ( $M = 100$  fully hidden sequences of length  $\ell = 1000$ ) corresponding to the fully labelled dataset  $\mathcal{P}_{infer.test}$ .

To generate the training sets, for each  $N \in \{1, 10, 100\}$ , we considered the appropriate precursor set  $\mathcal{P}_{N.infer.train}$  ( $N$  fully observed sequences of length  $T = 100$ ) depicted in Subsection 7.1.2.

We varied the mean labelling error probability  $\rho$  in  $\{0.1, 0.2, 0.3, 0.4, 0.5, 0.6, 0.7, 0.8, 0.9, 0.95\}$ . For  $N \in \{1, 10, 100\}$ , and each value of  $\rho$ , we generated 15 replicates from dataset  $\mathcal{P}_{N.infer.train}$ , each time varying

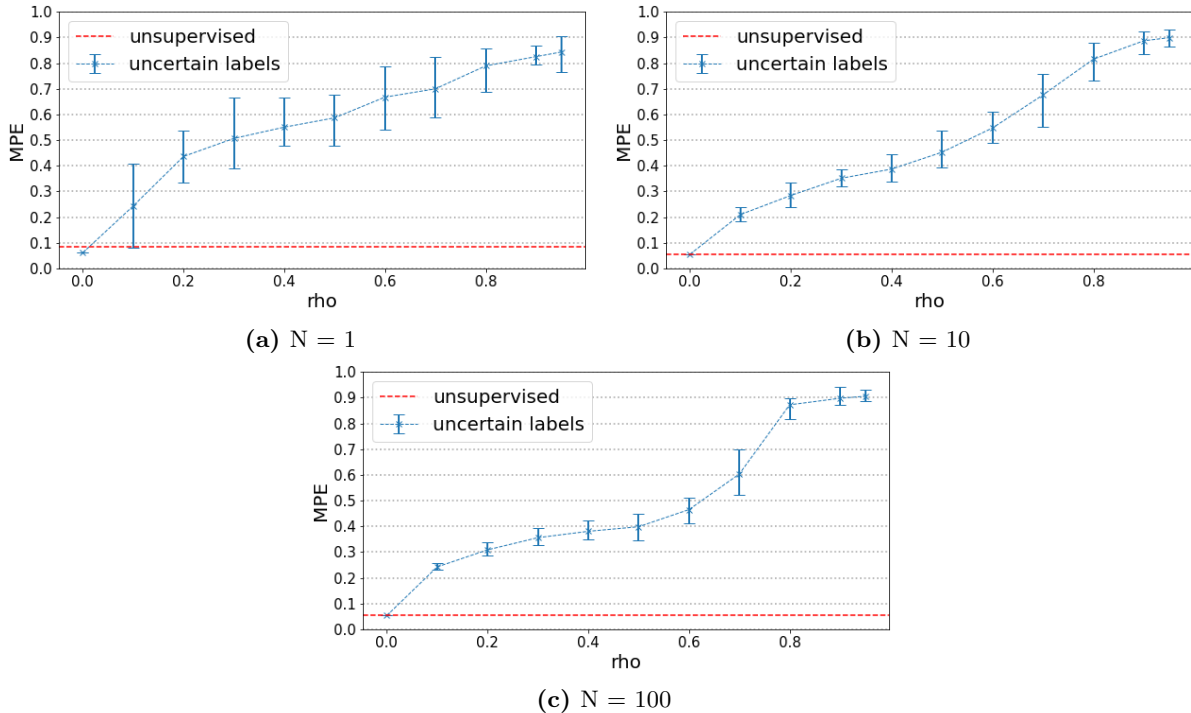


**Figure 8** 95% confidence interval for mean percentage error (MPE) of hidden state inference, as a function of the mean labelling error probability  $\rho$ . Models were trained on  $N$  sequences, for each of 15 replicates differing by the  $\rho\%$  ill-labelled observations. The average MPE was computed from the 15 replicates. The dash (red) line indicates the MPE score obtained for the unsupervised learning case. Mind the differences in scales between the three subfigures.

the distribution of the wrong labels amongst the observations. The PHMC-LAR(2) model with 4 states was trained on each of the training sets  $\mathcal{S}_{N,\rho,infer\_train_1}, \dots, \mathcal{S}_{N,\rho,infer\_train_{15}}$  thus obtained.

For each trained model, state inference was achieved, which yielded  $M = 100$  sequences of predicted labels of length 1000, to be compared with the label sequences within  $\mathcal{P}_{infer\_test}$  (see Subsection 7.1.1).

Figure 8 presents 95% confidence intervals for the MPE score as a function of  $\rho$ . Note that for all sizes  $N \in \{1, 10, 100\}$  of training data, the average MPE gradually increases when  $\rho$  tends to 1. Moreover, confidence intervals become more and more tight when larger training data is considered. We also observe that up to  $\rho = 0.7$ , the robustness to labelling errors, translated into small MPE average and low dispersion, increases with  $N$ . However, from  $\rho \geq 0.8$ , this trend is reversed and inference performance slightly decreases when  $N$  grows.

On the other hand, we underline that the fully unsupervised case outperforms supervised cases in presence of labelling errors. Up to relatively high labelling error rates ( $\rho = 70\%$ ), the trade-off between training time and inference performance becomes beneficial for large training datasets. For instance, for  $N = 100$ , with a 70%-reliable labelling function (*i.e.*  $\rho = 0.3$ ), the EM algorithm converges after a single iteration against 67 iterations for the unsupervised case; and the resulting model has good inference abilities with an MPE score equal to 35% on average (see Fig. 8c) against 5% on average in the unsupervised case. Thus, when analyzing real-world data for which the number of states  $K$  and auto-regressive order  $p$  are unknown, model selection strategies can capitalize on such labelling functions in order to explore/prospect larger grids of values for the hyperparameters  $K$  and  $p$ .

#### 7.4.2 Forecasting

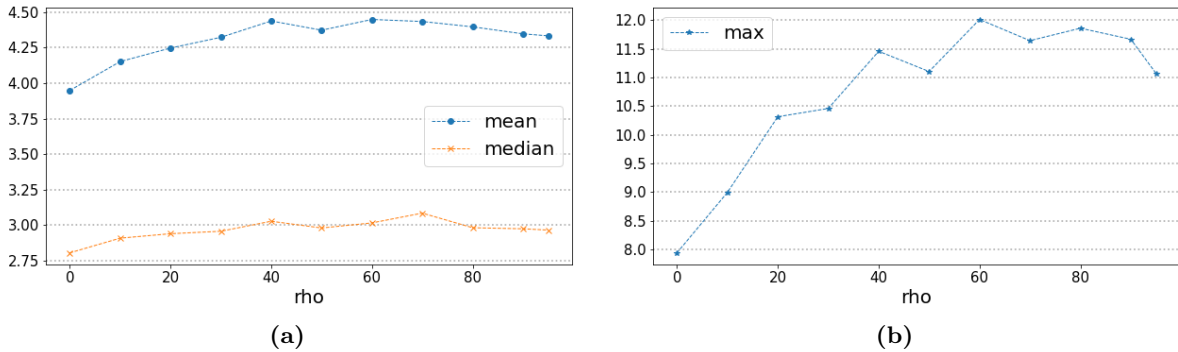
As in Subsection 7.3.2, we considered models trained on a single sequence ( $N = 1$ ). Again, for each value of the mean labelling error probability  $\rho$ , we used precursor set  $\mathcal{P}_{N=1,forecast\_train\_test}$  described in Subsection 7.1.2, and we varied the distribution of wrong labels: 15 replicates (*i.e.*, 15 sequences of length  $T = 100$ ) were thus generated. Out-of-sample forecasting was carried out at horizons  $T + h$ ,  $h = 1, \dots, 10$ .

Table 3 presents RMSE scores for different values of mean labelling error  $\rho$  when states are unknown at forecast horizons  $h = 1, \dots, 10$ . The results show that at forecast horizons  $h = 1, 2, 5, 6$ , the best prediction accuracies are reached when  $\rho$  is null, whereas at the remaining horizons, the highest accuracies are obtained when  $\rho = 0.8$  or 0.9. Figure 9 presents the mean, median and maximum for the prediction errors computed over the whole forecast

$\rho \backslash h$	1	2	3	4	5	6	7	8	9	10
0	<b>1.267</b>	<b>7.613</b>	1.447	3.076	<b>4.164</b>	<b>2.535</b>	1.132	7.937	7.854	2.464
0.1	1.814	8.992	1.393	3.193	4.334	2.625	1.117	7.865	7.780	2.407
0.2	2.258	10.315	1.529	2.855	4.758	3.026	0.811	7.481	7.398	2.044
0.3	2.793	10.458	1.575	2.911	4.689	3.004	0.801	7.512	7.426	2.062
0.4	2.877	11.457	1.161	3.114	4.779	2.941	0.886	7.562	7.478	2.123
0.5	2.655	11.104	1.396	2.953	4.812	3.008	0.843	7.488	7.410	2.062
0.6	2.925	12.013	1.004	3.031	4.878	3.002	0.749	7.472	7.392	2.020
0.7	3.088	11.643	1.271	2.969	4.901	3.082	0.706	7.409	7.321	1.954
0.8	2.656	11.860	<b>0.905</b>	3.001	4.848	2.954	0.768	7.498	7.422	2.046
0.9	2.444	11.667	1.338	<b>2.786</b>	5.011	3.164	<b>0.647</b>	<b>7.310</b>	<b>7.234</b>	<b>1.875</b>
0.95	2.362	11.071	1.192	3.027	4.685	2.905	0.866	7.588	7.504	2.135

**Table 3** Root mean square error (RMSE) of prediction at horizon  $h$  for different values of the mean labelling error probability  $\rho$ , when the states are unknown throughout forecast horizons. The forecast horizons are time-steps  $T + 1$  to  $T + h$ ,  $T = 100$ . The states are unknown from  $T + 1$  to  $T + 10$  time-steps. For a given value of  $\rho$ , models were each trained on a unique sequence: the sequence’s prefix of length  $T = 100$  was used for training, for each of 15 replicates differing by the position of ill-labelled observations distributed in the prefix. Then, out-of-sample forecasting was carried out at time-steps  $T + 1, \dots, T + 10$ , for the same sequence. The figures in bold highlight the minimum RMSE obtained across all mean labelling error probabilities ( $\rho$ ), at each horizon ( $h$ ) considered

horizons as a function of  $\rho$ . We observe that the mean and median very slightly increase with  $\rho$ , whereas labelling errors exert a greater impact on the maximum values of RMSEs. Therefore, this second experiment also highlights the remarkable robustness to error labelling in the prediction task, over the whole range of error rates.



**Figure 9** Descriptive statistics for the distribution of the root mean square error (RMSE) of prediction, as a function of  $\rho$ : (a) mean and median for prediction error, (b) maximum for prediction error.  $\rho$  denotes the mean labelling error probability. The forecast horizons are time-steps  $T + 1$  to  $T + h$ ,  $T = 100$ . The statistics are computed over all horizons.

## 8 Conclusion

In this work, we have introduced the PHMC-LAR model to analyze time series subject to switches in regimes. Our model is a generalization of the well-known Hidden Regime-switching Autoregressive (HRSAR) and Observed Regime-switching Autoregressive (ORSAR) models when regime-switching is modelled by a Markov Chain. Our model allows to handle the intermediate case where the state process is partially observed.

In the evaluation, we conducted our experiments on simulated data and considered both inference performance and prediction accuracy. The results show that the partially observed states (when they represent a reasonable proportion) allow a better characterization of training data (reflected by greater log-likelihood), in comparison with the unsupervised case. An interesting characteristics of the PHMC-LAR model is that the partially observed states allow faster convergence for the learning algorithm. This performance is obtained with no or practically no impact on the quality of hidden state inference, as from labelling percentages around 20%-30%; the prediction accuracy is also preserved above such percentage thresholds. Furthermore, faster EM convergence is also verified in a fully supervised scheme where part of the observations is ill-labelled. Model selection strategies can therefore rely on an approximate labelling function (provided by an expert or by a supervised algorithm learnt on a small subset of data for which the true labels are known), to explore larger grids of hyperparameter values. In addition, complementary experimental studies have revealed the robustness of our model to labelling errors, particularly when large training datasets and moderate labelling error rates are considered. Finally, we showed the ability of our variant of the Viterbi algorithm to infer partially-labelled sequences.

A natural extension of the PHMC-LAR model consists in putting uncertainty on partial knowledge: for instance instead of states observed with no doubt, a subset of possible states with various occurrence probabilities can be considered at each time-step. On the other hand, it is more realistic to consider time-dependent state processes, especially when large time series are analyzed. These directions will be investigated in future work.

## Acknowledgements

The software development and the realization of the experiments were performed at the CCIPL (Centre de Calcul Intensif des Pays de la Loire, Nantes, France).

## Funding

Fatoumata Dama is supported by a PhD scholarship granted by the French Ministry for Higher Education, Research and Innovation.

## A Appendix: backward-forward-backward algorithm

The *Backward-forward-backward* algorithm introduced by [Scheffer and Wrobel \(2001\)](#) for PHMC model learning has been adapted to the PHMC-LAR framework. This algorithm makes it possible to compute the probabilities

$$\xi_t(k, \ell) = P(S_{t-1} = k, S_t = \ell | X_{1-p}^T = x_{1-p}^T, \Sigma; \hat{\theta}), \quad \text{for } t = 2, \dots, T, \quad 1 \leq k, \ell \leq K \quad (36)$$

in  $\mathcal{O}(TK^2)$  operations. The analytical development for the above quantity involves three additional probabilities:

$$\xi_t(k, \ell) = \frac{\beta_t(\ell) P(S_t = \ell | S_{t-1} = k; \hat{\theta}) P(X_t = x_t | X_{t-p}^{t-1}, S_t = \ell; \hat{\theta}) \alpha_{t-1}(k) \tau_t(\ell)}{P(X_1^T = x_1^T | X_{1-p}^0, \Sigma; \hat{\theta}) \tau_{t-1}(k)} \times \mathbf{1}_{\{\ell \in \sigma_t, k \in \sigma_{t-1}\}}, \quad (37)$$

with

$$\begin{aligned} \tau_t(s) &= P(\sigma_{t+1}, \dots, \sigma_T | S_t = s, \hat{\theta}), \\ \alpha_t(s) &= P(S_t = s, X_1^t = x_1^t | X_{1-p}^0, \Sigma; \hat{\theta}), \\ \beta_t(s) &= P(X_{t+1}^T = x_{t+1}^T | X_{t+1-p}^t, S_t = s, \Sigma; \hat{\theta}). \end{aligned}$$

The algorithm operates recursively in three steps: two backward steps chained through a forward step. The first backward step computes the set of probabilities  $\tau_t(s)$  (subsection [A.1](#)); the forward step computes probabilities  $\alpha_t(s)$  (subsection [A.2](#)); the second backward step computes probabilities  $\beta_t(s)$ . In subsection [A.4](#), we describe a scaling method that is necessary to prevent floating point underflow when running the algorithm, especially when large sequences are considered.

**Proof.** First, in Eq. 38, the conditional probability is transformed into a joint probability. Then, in Eq. 39, we successively marginalize  $X_{t+1}^T$ ,  $X_t$ ,  $S_t$  and  $(S_{t-1}, X_1^{t-1})$ . According to the conditional independence graph of the PHMC-LAR model, the marginalization of  $X_{t+1}^T$  gives  $\beta_t(\ell)$ , that of  $X_t$  yields  $P(X_t = x_t | S_t = \ell, X_{t-p}^{t-1}, \Sigma; \hat{\theta})$ , that of  $S_t$  gives  $P(S_t = \ell | S_{t-1} = k, \Sigma; \hat{\theta})$  and that of  $(S_{t-1}, X_1^{t-1})$  provides  $\alpha_{t-1}(k)$ . Finally, in Eq. 41-43, the probability  $P(S_t = \ell | S_{t-1} = k, \Sigma; \hat{\theta})$  is developed using Bayes' rule. Note that in Eq. 43, the probability  $P(S_t = \ell, \sigma_t | S_{t-1} = k, \sigma_{t-1}; \hat{\theta})$  is null for  $\ell \notin \sigma_t$  and is not defined for  $k \notin \sigma_{t-1}$ .

$$\begin{aligned} \xi_t(k, \ell) &= P(S_{t-1} = k, S_t = \ell | X_{1-p}^T = x_{1-p}^T, \Sigma; \hat{\theta}) \\ &= \frac{P(S_{t-1} = k, S_t = \ell, X_1^T | X_{1-p}^0, \Sigma; \hat{\theta})}{P(X_1^T | X_{1-p}^0, \Sigma; \hat{\theta})} \end{aligned} \quad (38)$$

$$\begin{aligned} &= P(X_{t+1}^T = x_{t+1}^T | S_{t-1} = k, S_t = \ell, X_1^T, X_{1-p}^0, \Sigma; \hat{\theta}) \\ &\quad \times P(X_t = x_t | S_{t-1} = k, S_t = \ell, X_1^{t-1}, X_{1-p}^0, \Sigma; \hat{\theta}) \\ &\quad \times P(S_t = \ell | S_{t-1} = k, X_1^{t-1}, X_{1-p}^0, \Sigma; \hat{\theta}) \frac{P(S_{t-1} = k, X_1^{t-1} = x_1^{t-1} | X_{1-p}^0, \Sigma; \hat{\theta})}{P(X_1^T | X_{1-p}^0, \Sigma; \hat{\theta})} \end{aligned} \quad (39)$$

$$= \frac{\beta_t(\ell) P(X_t = x_t | S_t = \ell, X_{t-p}^{t-1}, \Sigma; \hat{\theta}) \alpha_{t-1}(k)}{P(X_1^T | X_{1-p}^0, \Sigma; \hat{\theta})} \times P(S_t = \ell | S_{t-1} = k, \Sigma; \hat{\theta}) \quad (40)$$

with

$$P(S_t = \ell | S_{t-1} = k, \Sigma; \hat{\theta}) = \frac{P(S_t = \ell, S_{t-1} = k, \sigma_1^T; \hat{\theta})}{P(S_{t-1} = k, \sigma_1^T; \hat{\theta})} \quad (41)$$

$$= \frac{P(\sigma_{t+1}^T | S_t = \ell, S_{t-1} = k, \sigma_1^t; \hat{\theta}) P(S_t = \ell, S_{t-1} = k, \sigma_1^t; \hat{\theta})}{P(\sigma_t^T | S_{t-1} = k, \sigma_1^{t-1}; \hat{\theta}) P(S_{t-1} = k, \sigma_1^{t-1}; \hat{\theta})} \quad (42)$$

$$\begin{aligned} &= \frac{\tau_t(\ell)}{\tau_{t-1}(k)} \times P(S_t = \ell, \sigma_t | S_{t-1} = k, \sigma_{t-1}; \hat{\theta}) \\ &= \begin{cases} \frac{\tau_t(\ell)}{\tau_{t-1}(k)} \times P(S_t = \ell | S_{t-1} = k; \hat{\theta}) & \text{if } k \in \sigma_{t-1}, \ell \in \sigma_t \\ 0 & \text{otherwise} \end{cases} \end{aligned} \quad (43)$$

## A.1 First backward step

The first backward step computes probabilities  $\tau_t(s)$ , the probabilities of the remaining possible states given that state  $s \in \{1, \dots, K\}$  is observed at time-step  $t \in \{1, \dots, T\}$ :  $\tau_t(s) = P(\sigma_{t+1}, \dots, \sigma_T | S_t = s, \hat{\theta}) = P(S_{t+1} \in \sigma_{t+1}, \dots, S_T \in \sigma_T | S_t = s, \hat{\theta})$ . This set of probabilities is computed recursively as follows:

$$\begin{cases} \tau_T(s) := 1 \\ \tau_t(s) = \sum_{i \in \sigma_{t+1}} \tau_{t+1}(i) P(S_{t+1} = i | S_t = s; \hat{\theta}). \end{cases} \quad (44)$$

**Proof.** *Base case:*  $t = T - 1$

By applying the definition of  $\tau_{T-1}$ , we obtain:

$$\tau_{T-1}(s) = P(\sigma_T | S_{T-1} = s, \hat{\theta}) = P(S_T \in \sigma_T | S_{T-1} = s; \hat{\theta}) \quad (45)$$

$$= \sum_{i \in \sigma_T} \tau_T(i) P(S_T = i | S_{T-1} = s; \hat{\theta}). \quad (46)$$

*Recursive case:*  $t = T - 2, \dots, 1$

We first use the law of total probabilities (Eq. 47), followed by Bayes' rule (Eq. 48). Note that in Eq. 48, the probability  $P(\sigma_{t+1}, \dots, \sigma_T | S_{t+1} = i, S_t = s, \hat{\theta})$  is null for  $i \notin \sigma_{t+1}$  (since  $\sigma_{t+1}$  is the set of possible states at

time-step  $t + 1$ ); otherwise it equals  $P(\sigma_{t+2}, \dots, \sigma_T | S_{t+1} = i, \hat{\theta}) = \tau_{t+1}(i)$  (Eq. 49). Thus, we obtain the recursive formula presented in Eq. 44.

$$\begin{aligned} \tau_t(s) &= P(\sigma_{t+1}, \dots, \sigma_T | S_t = s, \hat{\theta}) \\ &= \sum_{i=1}^K P(\sigma_{t+1}, \dots, \sigma_T, S_{t+1} = i | S_t = s, \hat{\theta}) \end{aligned} \quad (47)$$

$$= \sum_{i=1}^K P(\sigma_{t+1}, \dots, \sigma_T | S_{t+1} = i, S_t = s, \hat{\theta}) P(S_{t+1} = i | S_t = s, \hat{\theta}) \quad (48)$$

$$= \sum_{i \in \sigma_{t+1}} P(\sigma_{t+2}, \dots, \sigma_T | S_{t+1} = i, \hat{\theta}) P(S_{t+1} = i | S_t = s, \hat{\theta}) \quad (49)$$

$$= \sum_{i \in \sigma_{t+1}} \tau_{t+1}(i) P(S_{t+1} = i | S_t = s, \hat{\theta}) \quad (50)$$

## A.2 Forward step

This step allows to compute the probabilities of being in regime  $s$  at time-step  $t$  while observing sequence  $x_1, \dots, x_t$ . These probabilities, denoted by  $\alpha_t(s)$ , are defined as  $\alpha_t(s) = P(S_t = s, X_1^t = x_1^t | X_{1-p}^0, \Sigma; \hat{\theta})$  for  $1 \leq t \leq T$ ,  $1 \leq s \leq K$ . They are computed as follows:

$$\begin{cases} \alpha_1(s) = P(X_1 = x_1 | X_{1-p}^0, S_1 = s; \hat{\theta}) P(S_1 = s; \hat{\theta}) \frac{\tau_1(s)}{\sum_{i \in \sigma_1} \tau_1(i) P(S_1 = i; \hat{\theta})} \\ \alpha_t(s) = P(X_t = x_t | X_{t-p}^{t-1}, S_t = s; \hat{\theta}) \sum_{i \in \sigma_{t-1}} \alpha_{t-1}(i) P(S_t = s | S_{t-1} = i; \hat{\theta}) \frac{\tau_t(s)}{\tau_{t-1}(i)} \times \mathbf{1}_{\{s \in \sigma_t\}} \end{cases} \quad (51)$$

To note, the likelihood of sequence  $x_1^T$  can be easily computed by integrating out  $S_t$  in  $\alpha_T$ :

$$P(X_1^T = x_1^T | X_{1-p}^0; \hat{\theta}) = \sum_{s=1}^K \alpha_T(s). \quad (52)$$

The likelihood of  $N$  independent sequences is therefore calculated by multiplying the individual likelihoods across the sequences.

**Proof.** *Base case:  $t = 1$*

In Eq. 53, using the conditional independence graph of the PHMC-LAR model, we transform the joint probability into two conditional probabilities,  $P(X_1 = x_1 | S_1 = s, X_{1-p}^0; \hat{\theta})$  and  $P(S_1 = s | \Sigma; \hat{\theta})$ . Then, in Eq. 54, Bayes' rule is applied to the latter conditional probability. It can be easily shown that  $P(\Sigma; \hat{\theta}) = \sum_{i \in \sigma_1} \tau_1(i) P(S_1 = i; \hat{\theta})$ . Thus we obtain Eq. 55.

$$\begin{aligned} \alpha_1(s) &= P(S_1 = s, X_1 = x_1 | X_{1-p}^0, \Sigma; \hat{\theta}) \\ &= P(X_1 = x_1 | S_1 = s, X_{1-p}^0; \hat{\theta}) \times P(S_1 = s | \Sigma; \hat{\theta}) \end{aligned} \quad (53)$$

$$= P(X_1 = x_1 | S_1 = s, X_{1-p}^0; \hat{\theta}) \times \frac{P(\sigma_1, \dots, \sigma_T | S_1 = s; \hat{\theta}) P(S_1 = s; \hat{\theta})}{P(\Sigma; \hat{\theta})} \quad (54)$$

$$= P(X_1 = x_1 | S_1 = s, X_{1-p}^0; \hat{\theta}) P(S_1 = s; \hat{\theta}) \frac{\tau_1(s)}{\sum_{i \in \sigma_1} \tau_1(i) P(S_1 = i; \hat{\theta})}. \quad (55)$$

*Recursive case:  $t = 2, \dots, T$*

As previously, the joint probability is split into two conditional probabilities (Eq. 56). We use the law of total probabilities to introduce  $S_{t-1}$  in Eq. 57. From Eq. 57 to Eq. 58, Bayes' rule is applied on the terms within the sum. Then, in Eq. 59, recursive terms  $\alpha_{t-1}$  weighted by probabilities  $P(S_t = s | S_{t-1} = i, \Sigma; \hat{\theta})$  appear within the sum. Finally, probabilities  $P(S_t = s | S_{t-1} = i, \Sigma; \hat{\theta})$  are computed through the calculations presented in Eq. 60-63. Thus, by substituting Eq. 63 in Eq. 59, we obtain the recursive case (Eq. 51).

$$\begin{aligned}\alpha_t(s) &= P(S_t = s, X_1^t = x_1^t | X_{1-p}^0, \Sigma; \hat{\theta}) \\ &= P(X_t = x_t | X_1^{t-1}, S_t = s, X_{1-p}^0, \Sigma; \hat{\theta}) \times P(X_1^{t-1} = x_1^{t-1}, S_t = s | X_{1-p}^0, \Sigma; \hat{\theta})\end{aligned}\quad (56)$$

$$\begin{aligned}&= P(X_t = x_t | X_{t-p}^{t-1}, S_t = s; \hat{\theta}) \\ &\quad \sum_{i=1}^K P(X_1^{t-1} = x_1^{t-1}, S_t = s, S_{t-1} = i | X_{1-p}^0, \Sigma; \hat{\theta})\end{aligned}\quad (57)$$

$$\begin{aligned}&= P(X_t = x_t | X_{t-p}^{t-1}, S_t = s; \hat{\theta}) \\ &\quad \sum_{i=1}^K P(X_1^{t-1} = x_1^{t-1}, S_{t-1} = i | X_{1-p}^0, \Sigma; \hat{\theta}) P(S_t = s | S_{t-1} = i, \Sigma; \hat{\theta})\end{aligned}\quad (58)$$

$$= P(X_t = x_t | X_{t-p}^{t-1}, S_t = s; \hat{\theta}) \sum_{i=1}^K \alpha_{t-1}(i) P(S_t = s | S_{t-1} = i, \Sigma; \hat{\theta})\quad (59)$$

where

$$P(S_t = s | S_{t-1} = i, \Sigma; \hat{\theta}) = \frac{P(S_t = s, S_{t-1} = i, \Sigma; \hat{\theta})}{P(S_{t-1} = i, \Sigma; \hat{\theta})}\quad (60)$$

$$\begin{aligned}&= \frac{P(\sigma_{t+1}, \dots, \sigma_T | S_t = s, S_{t-1} = i, \sigma_1^t; \hat{\theta})}{P(\sigma_t, \dots, \sigma_T | S_{t-1} = i, \sigma_1^{t-1}; \hat{\theta}) P(S_{t-1} = i, \sigma_1^{t-1}; \hat{\theta})} \\ &\quad \times P(S_t = s, \sigma_t | S_{t-1} = i, \sigma_1^{t-1}; \hat{\theta}) P(S_{t-1} = i, \sigma_1^{t-1}; \hat{\theta})\end{aligned}\quad (61)$$

$$= \frac{\tau_t(s)}{\tau_{t-1}(i)} \times P(S_t = s, \sigma_t | S_{t-1} = i, \sigma_{t-1}; \hat{\theta})\quad (62)$$

$$= \frac{\tau_t(s)}{\tau_{t-1}(i)} \times \begin{cases} P(S_t = s | S_{t-1} = i; \hat{\theta}) & \text{if } i \in \sigma_{t-1}, s \in \sigma_t \\ 0 & \text{otherwise.} \end{cases}\quad (63)$$

### A.3 Second backward step

In this second backward step, quantities  $\beta_t(s) = P(X_{t+1}^T = x_{t+1}^T | X_{t+1-p}^t, S_t = s, \Sigma; \hat{\theta})$  are computed.  $\beta_t(s)$  denotes the probability to observe sequence  $x_{t+1}, \dots, x_T$  given that state  $s$  has been observed at time-step  $t$ . These probabilities are recursively computed as follows:

$$\begin{cases} \beta_T(s) := 1 \\ \beta_t(s) = \sum_{i \in \sigma_{t+1}} \beta_{t+1}(i) P(S_{t+1} = i | S_t = s; \hat{\theta}) \frac{\tau_{t+1}(i)}{\tau_t(s)} \\ \quad P(X_{t+1} = x_{t+1} | X_{t+1-p}^t, S_{t+1} = i; \hat{\theta}) \times \mathbf{1}_{\{s \in \sigma_t\}}. \end{cases}\quad (64)$$

**Proof.** *Base case:*  $t = T - 1$

Equation 65 is obtained by applying the law of total probabilities. In Eq. 66, Bayes' rule is applied to  $P(S_T = i | S_{T-1} = s, \Sigma; \hat{\theta})$  and a quotient of probabilities appears. Then, the numerator and denominator of this quotient are transformed into products of conditional probabilities (Eq. 67). In Eq. 68, we introduce backward propagation terms  $\beta_T(i)$  and  $\tau_T(i)$ , which each equal one (by definition); thanks to Markov property, probability  $P(S_T = i, \sigma_T | S_{T-1} = s, \sigma_1, \dots, \sigma_{T-1}; \hat{\theta})$  is equal to  $P(S_T = i | S_{T-1} = s; \hat{\theta})$  if  $i \in \sigma_T$  and  $s \in \sigma_{T-1}$ , and this probability is null if  $i \notin \sigma_T$  and is undefined if  $s \notin \sigma_{T-1}$  (hence the indicator function  $\mathbf{1}_{\{s \in \sigma_{T-1}, i \in \sigma_T\}}$ ). Besides, in Eq. 67, a common term appears at numerator and denominator, which entails a simplification. Finally, probability  $P(\sigma_T | S_{T-1} = s, \sigma_1, \dots, \sigma_{T-1}; \hat{\theta})$  appearing at denominator equals  $\tau_{T-1}(s)$  thanks to Markov property.

$$\begin{aligned}\beta_{T-1}(s) &= P(X_T = x_T | X_{T-p}^{T-1}, S_{T-1} = s, \Sigma; \hat{\theta}) \\ &= \sum_{i=1}^K P(X_T = x_T | X_{T-p}^{T-1}, S_T = i, \Sigma; \hat{\theta}) P(S_T = i | S_{T-1} = s, \Sigma; \hat{\theta})\end{aligned}\quad (65)$$

$$= \sum_{i=1}^K P(X_T = x_T | X_{T-p}^{T-1}, S_T = i; \hat{\theta}) \frac{P(S_T = i, S_{T-1} = s, \Sigma; \hat{\theta})}{P(S_{T-1} = s, \Sigma; \hat{\theta})}\quad (66)$$

$$\begin{aligned}&= \sum_{i=1}^K P(X_T = x_T | X_{T-p}^{T-1}, S_T = i; \hat{\theta}) \\ &\quad \times \frac{P(S_T = i, \sigma_T | S_{T-1} = s, \sigma_1, \dots, \sigma_{T-1}; \hat{\theta}) P(S_{T-1} = s, \sigma_1, \dots, \sigma_{T-1}; \hat{\theta})}{P(\sigma_T | S_{T-1} = s, \sigma_1, \dots, \sigma_{T-1}; \hat{\theta}) P(S_{T-1} = s, \sigma_1, \dots, \sigma_{T-1}; \hat{\theta})}\end{aligned}\quad (67)$$

$$\begin{aligned}&= \sum_{i=1}^K \beta_T(i) P(X_T = x_T | X_{T-p}^{T-1}, S_T = i; \hat{\theta}) \frac{\tau_T(i)}{\tau_{T-1}(s)} \\ &\quad \times P(S_T = i | S_{T-1} = s; \hat{\theta}) \times \mathbf{1}_{\{s \in \sigma_{T-1}, i \in \sigma_T\}}.\end{aligned}\quad (68)$$

*Recursive case:*  $t = T - 2, \dots, 1$

The application of the law of total probabilities yields Eq. 69. In Eq. 70,  $X_{t+2}^T$  then  $X_{t+1}$  are marginalized, which allows to make appear the recursive term  $\beta_{t+1}$  together with the conditional probability of  $X_{t+1}$  given  $S_{t+1}$  and past values in Eq. 71. As in the base case, probability  $P(S_{t+1} = i | S_t = s, \Sigma; \hat{\theta})$  is computed using Bayes' rule (Eq. 72-75).

$$\begin{aligned}\beta_t(s) &= P(X_{t+1}^T = x_{t+1}^T | X_{t+1-p}^t, S_t = s, \Sigma; \hat{\theta}) \\ &= \sum_{i=1}^K P(X_{t+1} = x_{t+1}, X_{t+2}^T = x_{t+2}^T, S_{t+1} = i | X_{t+1-p}^t, S_t = s, \Sigma; \hat{\theta})\end{aligned}\quad (69)$$

$$\begin{aligned}&= \sum_{i=1}^K P(X_{t+2}^T = x_{t+2}^T | X_{t+1-p}^{t+1}, S_{t+1} = i, \Sigma; \hat{\theta}) \\ &\quad \times P(X_{t+1} = x_{t+1} | X_{t+1-p}^t, S_{t+1} = i, \Sigma; \hat{\theta}) P(S_{t+1} = i | S_t = s, \Sigma; \hat{\theta})\end{aligned}\quad (70)$$

$$= \sum_{i=1}^K \beta_{t+1}(i) P(X_{t+1} = x_{t+1} | X_{t+1-p}^t, S_{t+1} = i, \Sigma; \hat{\theta}) P(S_{t+1} = i | S_t = s, \Sigma; \hat{\theta})\quad (71)$$

where

$$P(S_{t+1} = i | S_t = s, \Sigma; \hat{\theta}) = \frac{P(S_{t+1} = i, S_t = s, \Sigma; \hat{\theta})}{P(S_t = s, \Sigma; \hat{\theta})}\quad (72)$$

$$\begin{aligned}&= (\sigma_{t+2}, \dots, \sigma_T | S_{t+1} = i, S_t = s, \sigma_1, \dots, \sigma_{t+1}; \hat{\theta}) \times \\ &\quad \frac{P(S_{t+1} = i, \sigma_{t+1} | S_t = s, \sigma_1, \dots, \sigma_t; \hat{\theta}) P(S_t = s, \sigma_1, \dots, \sigma_t; \hat{\theta})}{P(\sigma_{t+1}, \dots, \sigma_T | S_t = s, \sigma_1, \dots, \sigma_t; \hat{\theta}) P(S_t = s, \sigma_1, \dots, \sigma_t; \hat{\theta})}\end{aligned}\quad (73)$$

$$= \frac{\tau_{t+1}(i)}{\tau_t(s)} \times P(S_{t+1} = i, \sigma_{t+1} | S_t = s, \sigma_t; \hat{\theta})\quad (74)$$

$$= \frac{\tau_{t+1}(i)}{\tau_t(s)} \times P(S_{t+1} = i | S_t = s; \hat{\theta}) \times \mathbf{1}_{\{s \in \sigma_t, i \in \sigma_{t+1}\}}.\quad (75)$$

#### A.4 Scaling of backward-forward-backward algorithm

For large sequences, *i.e.* large value of  $T$ , the quantities  $\tau_t(s)$ ,  $\alpha_t(s)$  and  $\beta_t(s)$  tend to zero as products of probabilities. Thus, the computations will require beyond the precision range of machine and PHMC-LAR parameter estimate will be inaccurate. Generally, this problem is solved by normalizing  $\tau_t(s)$ ,  $\alpha_t(s)$  and  $\beta_t(s)$  by a term of



same order of magnitude (Florez-Larrahondo, 2020; Koenig and Simmons, 1996). Thus, we propose the following normalization:

$$\tilde{\tau}_t(s) = \frac{\tau_t(s)}{P(\sigma_t, \dots, \sigma_T | \sigma_{t-1}; \hat{\theta})}, \quad (76)$$

$$\tilde{\alpha}_t(s) = \frac{\alpha_t(s)}{P(X_1^t = x_1^t | X_{1-p}^0, \Sigma; \hat{\theta})}, \quad (77)$$

$$\tilde{\beta}_t(s) = \frac{\beta_t(s)}{P(X_t^T = x_t^T | X_{1-p}^{t-1}, \Sigma; \hat{\theta})}. \quad (78)$$

As previously,  $\tilde{\tau}_t(s)$ ,  $\tilde{\alpha}_t(s)$  and  $\tilde{\beta}_t(s)$  can be computed recursively. The recursive formula for these quantities can be deduced from those of  $\tau_t(s)$  (Eq. 44),  $\alpha_t(s)$  (Eq. 51) and  $\beta_t(s)$  (Eq. 64). To do so, Eq. 44, 51 and 64 are respectively divided by the normalization terms  $P(\sigma_t, \dots, \sigma_T | \sigma_{t-1}; \hat{\theta})$ ,  $P(X_1^t = x_1^t | X_{1-p}^0, \Sigma; \hat{\theta})$  and  $P(X_t^T = x_t^T | X_{1-p}^{t-1}, \Sigma; \hat{\theta})$ . After decomposing the formula obtained and after some calculations, we obtain the subsequent recursive formulas for  $\tilde{\tau}_t$ ,  $\tilde{\alpha}_t$  and  $\tilde{\beta}_t$ .

### First backward propagation

$$\begin{cases} \tilde{\tau}_T(s) = \frac{1}{P(\sigma_T | \sigma_{T-1}; \hat{\theta})} \\ \tilde{\tau}_t(s) = \sum_{i \in \sigma_{t+1}} \tilde{\tau}_{t+1}(i) \frac{P(S_{t+1} = i | S_t = s; \hat{\theta})}{P(\sigma_t | \sigma_{t-1}; \hat{\theta})}, \quad \text{for } t = T-1, \dots, 1, \end{cases} \quad (79)$$

with

$$\begin{aligned} P(\sigma_t | \sigma_{t-1}; \hat{\theta}) &= P(S_t \in \sigma_t | S_{t-1} \in \sigma_{t-1}; \hat{\theta}) = \sum_{i \in \sigma_{t-1}} \sum_{j \in \sigma_t} P(S_t = j | S_{t-1} = i; \hat{\theta}). \\ P(\sigma_1; \hat{\theta}) &= P(S_1 \in \sigma_1; \hat{\theta}) = \sum_{i \in \sigma_1} P(S_1 = i; \hat{\theta}). \end{aligned} \quad (80)$$

### Forward propagation

$$\begin{cases} \tilde{\alpha}_1(s) = \frac{P(X_1 = x_1 | X_{1-p}^0, S_1 = s; \hat{\theta}) P(S_1 = s; \hat{\theta})}{C_1} \times \frac{\tilde{\tau}_1(s)}{\sum_{i \in \sigma_1} \tilde{\tau}_1(i) P(S_1 = i; \hat{\theta})} \\ \tilde{\alpha}_t(s) = P(X_t = x_t | X_{t-p}^{t-1}, S_t = s; \hat{\theta}) \left[ \sum_{i \in \sigma_{t-1}} \tilde{\alpha}_{t-1}(i) P(S_t = s | S_{t-1} = i; \hat{\theta}) \frac{\tilde{\tau}_t(s)}{\tilde{\tau}_{t-1}(i)} \right] \\ \times \frac{1}{P(\sigma_{t-1} | \sigma_{t-2}; \hat{\theta}) C_t} \times \mathbf{1}_{\{s \in \sigma_t\}} \end{cases} \quad (81)$$

with  $P(\sigma_{t-1} | \sigma_{t-2}; \hat{\theta})$  defined in Eq. 80 and  $C_t$  the scaling term defined and computed as follows:

$$C_1 = P(X_1 = x_1 | X_{1-p}^0, \Sigma; \hat{\theta}) = \sum_{i \in \sigma_1} P(X_1 = x_1 | X_{1-p}^0, S_1 = i; \hat{\theta}) P(S_1 = i; \hat{\theta}) \quad (82)$$

$$C_t = P(X_t = x_t | X_{1-p}^{t-1}, \Sigma; \hat{\theta}) \quad \text{for } t = 2, \dots, T \quad (83)$$

$$= \sum_{s \in \sigma_t} P(X_t = x_t | X_{t-p}^{t-1}, S_t = s; \hat{\theta}) \times \left[ \sum_{i \in \sigma_{t-1}} \tilde{\alpha}_{t-1}(i) P(S_t = s | S_{t-1} = i; \hat{\theta}) \right]. \quad (84)$$

The proof is straightforward and is left to the reader. Note that  $P(X_1^T = x_1^T | X_{1-p}^0; \hat{\theta}) = \prod_{t=1}^T C_t$ .

## Second backward propagation

$$\left\{ \begin{array}{l} \tilde{\beta}_T(s) = \frac{1}{C_T} \\ \tilde{\beta}_t(s) = \sum_{i \in \sigma_{t+1}} \left[ \tilde{\beta}_{t+1}(i) P(S_{t+1} = i | S_t = s; \hat{\theta}) \frac{\tilde{\tau}_{t+1}(i)}{\tilde{\tau}_t(s)} P(X_{t+1} = x_{t+1} | X_{t+1-p}^t, S_{t+1} = i; \hat{\theta}) \right] \\ \times \frac{1}{P(\sigma_t | \sigma_{t-1}; \hat{\theta}) C_t} \times \mathbf{1}_{\{s \in \sigma_t\}} \end{array} \right. \quad (85)$$

where  $C_t$  and  $P(\sigma_t | \sigma_{t-1}; \hat{\theta})$  are defined in Eq. 82-83 and Eq. 80 respectively.

### $\xi_t(k, \ell)$ computation

In Eq. 36 probabilities  $\xi_t(k, \ell)$  are defined in function of quantities  $\tau_t, \tau_{t-1}, \alpha_{t-1}$  and  $\beta_t$ . These quantities can be easily expressed in function of their normalized versions  $\tilde{\tau}_t, \tilde{\tau}_{t-1}, \tilde{\alpha}_{t-1}$  and  $\tilde{\beta}_t$  using Eq. 76, 77 and 78. After substituting  $\tau_t, \tau_{t-1}, \alpha_{t-1}$  and  $\beta_t$  by the resulting expressions and after some simplifications, we obtain the following formula:

$$\xi_t(k, \ell) = \frac{\tilde{\beta}_t(\ell) P(S_t = \ell | S_{t-1} = k; \hat{\theta}) P(X_t = x_t | X_{t-p}^{t-1}, S_t = \ell; \hat{\theta}) \tilde{\alpha}_{t-1}(k) \tilde{\tau}_t(\ell)}{P(\sigma_{t-1} | \sigma_{t-2}; \hat{\theta}) \tilde{\tau}_{t-1}(k)} \times \mathbf{1}_{\{\ell \in \sigma_t, k \in \sigma_{t-1}\}}. \quad (86)$$

## B Appendix: decomposition of $Q(\theta, \hat{\theta}_{n-1})$

From Eq. 6 and 15, it is straightforward to show that  $Q(\theta, \hat{\theta}_{n-1})$  can be decomposed as the sum of quantities  $Q_S(\theta^{(S)}, \hat{\theta}_{n-1})$  and  $Q_X(\theta^{(X)}, \hat{\theta}_{n-1})$ :

$$\begin{aligned} Q_S(\theta^{(S)}, \hat{\theta}_{n-1}) &= \sum_{i=1}^N \sum_{s \in \mathbf{K}} \ln \left( P(S_1^{(i)} = s; \hat{\theta}_{n-1}) \right) P(S_1^{(i)} = s | [X^{(i)}]_{1-p}^{T_i}, \Sigma^{(i)}; \hat{\theta}_{n-1}) \\ &+ \sum_{i=1}^N \sum_{t=2}^{T_i} \sum_{(s, s') \in \mathbf{K}^2} \ln \left( P(S_t^{(i)} = s | S_{t-1}^{(i)} = s'; \theta^{(S)}) \right) \\ &P(S_t^{(i)} = s, S_{t-1}^{(i)} = s' | [X^{(i)}]_{1-p}^{T_i}, \Sigma^{(i)}; \hat{\theta}_{n-1}), \end{aligned} \quad (87)$$

$$\begin{aligned} Q_X(\theta^{(X)}, \hat{\theta}_{n-1}) &= \sum_{i=1}^N \sum_{t=1}^{T_i} \sum_{s \in \mathbf{K}} \ln \left( P(x_t^{(i)} | X_{t-1}^{(i)}, \dots, X_{t-p}^{(i)}, S_t^{(i)} = s; \theta^{(X)}) \right) \\ &P(S_t^{(i)} = s | [X^{(i)}]_{1-p}^{T_i}, \Sigma^{(i)}; \hat{\theta}_{n-1}), \end{aligned} \quad (88)$$

with  $\mathbf{K} = \{1, \dots, K\}$ .

## References

- Ailliot P, Bessac J, Monbet V, Pene F (2015) Non-homogeneous hidden markov-switching models for wind time series. *Journal of Statistical Planning and Inference* 160:75–88
- Baum LE, Petrie T, Soules G, Weiss N (1970) A maximization technique occurring in the statistical analysis of probabilistic functions of markov chains. *The annals of mathematical statistics* 41(1):164–171
- Berg J, Reckordt T, Richter C, Reinhart G (2018) Action recognition in assembly for human-robot-cooperation using Hidden Markov Models. *Procedia CIRP* 76:205–210
- Bergmeir C, Hyndman RJ, Benítez JM (2016) Bagging exponential smoothing methods using STL decomposition and Box–Cox transformation. *International Journal of Forecasting* 32(2):303–312

- Bessac J, Ailliot P, Cattiaux J, Monbet V (2016) Comparison of hidden and observed regime-switching autoregressive models for (u, v)-components of wind fields in the Northeast Atlantic. *Advances in Statistical Climatology, Meteorology and Oceanography* 2(1):1–16
- Box GE, Jenkins GM, Reinsel GC, Ljung GM (2015) *Time series analysis: forecasting and control*, 5th edn. Wiley
- Cardenas-Gallo I, Sanchez-Silva M, Akhavan-Tabatabaei R, Bastidas-Arteaga E (2016) A Markov regime-switching framework application for describing El Niño Southern Oscillation (ENSO) patterns. *Natural Hazards* 81(2):829–843
- Clements MP, Krolzig HM (1998) A comparison of the forecast performance of markov-switching and threshold autoregressive models of US GNP. *The Econometrics Journal* 1(1):47–75
- Degtyarev AB, Gankevich I (2019) Evaluation of hydrodynamic pressures for autoregressive model of irregular waves. In: *Contemporary Ideas on Ship Stability*, Springer, pp 37–47
- Dempster AP, Laird NM, Rubin DB (1977) Maximum likelihood from incomplete data via the EM algorithm. *Journal of the Royal Statistical Society: Series B (Methodological)* 39(1):1–22
- Dickey DA, Fuller WA (1979) Distribution of the estimators for autoregressive time series with a unit root. *Journal of the American Statistical Association* 74(366):427–431
- Filardo AJ (1994) Business-cycle phases and their transitional dynamics. *Journal of Business & Economic Statistics* 12(3):299–308
- Florez-Larrahondo G (2020) Incremental learning of discrete hidden Markov models. PhD thesis, Mississippi State University
- Forney GD (1973) The Viterbi algorithm. *Proceedings of the IEEE* 61(3):268–278
- Gardner Jr E, Everette S (2006) Exponential smoothing: The state of the art - Part ii. *International Journal of Forecasting* 22(4):637–666
- Ghasvarian Jahromi K, Gharavian D, Mahdiani H (2020) A novel method for day-ahead solar power prediction based on hidden Markov model and cosine similarity. *Soft Computing* 24(7):4991–5004
- Hamilton JD (1989) A new approach to the economic analysis of nonstationary time series and the business cycle. *Econometrica* pp 357–384
- Hamilton JD (1990) Analysis of time series subject to changes in regime. *Journal of econometrics* 45(1-2):39–70
- Kim CJ (1994) Dynamic linear models with Markov-switching. *Journal of Econometrics* 60:1–22
- Koenig S, Simmons RG (1996) Unsupervised learning of probabilistic models for robot navigation. In: *Proceedings of IEEE International Conference on Robotics and Automation*, IEEE, vol 3, pp 2301–2308
- Kwiatkowski D, Phillips PC, Schmidt P, Shin Y (1992) Testing the null hypothesis of stationarity against the alternative of a unit root: How sure are we that economic time series have a unit root? *Journal of econometrics* 54(1-3):159–178
- Li K, Fu Y (2012) ARMA-HMM: a new approach for early recognition of human activity. In: 21st International Conference on Pattern Recognition (ICPR), pp 1779–1782
- Michalek S, Wagner M, Timmer J (2000) A new approximate likelihood estimator for ARMA-filtered Hidden Markov Models. *IEEE Transactions on Signal Processing* 48(6):1537–1547
- Morwal S, Jahan N, Chopra D (2012) Named entity recognition using hidden Markov model (HMM). *International Journal on Natural Language Computing (IJNLC)* 1(4):15–23
- Mouhcine R, Mustapha A, Zouhir M (2018) Recognition of cursive Arabic handwritten text using embedded training based on HMMs. *Journal of Electrical Systems and Information Technology* 5(2):245–251
- Noman F, Alkawsy G, Alkahtani AA, Al-Shetwi AQ, Tiong SK, Alalwan N, Ekanayake J, Alzahrani AI (2020) Multistep short-term wind speed prediction using nonlinear auto-regressive neural network with exogenous variable selection. *Alexandria Engineering Journal*

- Phillips PC, Perron P (1988) Testing for a unit root in time series regression. *Biometrika* 75(2):335–346
- Ramasso E, Denoeux T (2013) Making use of partial knowledge about hidden states in HMMs: an approach based on belief functions. *IEEE Transactions on Fuzzy Systems* 22(2):395–405
- Scheffer T, Wrobel S (2001) Active learning of partially hidden markov models. In: *Proceedings of the ECML/PKDD Workshop on Instance Selection*, Citeseer
- Schuller B, Rigoll G, Lang M (2003) Hidden Markov model-based speech emotion recognition. In: *IEEE International Conference on Multimedia and Expo (ICME)*, pp 401–404
- Ubilava D, Helmers CG (2013) Forecasting ENSO with a smooth transition autoregressive model. *Environmental modelling & software* 40:181–190
- Wang P, Wang H, Yan R (2019) Bearing degradation evaluation using improved cross recurrence quantification analysis and nonlinear auto-regressive neural network. *IEEE Access* 7:38937–38946
- Wold H (1954) A study in the analysis of stationary time series, vol Second revised edition. *Almqvist and Wiksell Book Co., Uppsala*
- Yu L, Zhou L, Tan L, Jiang H, Wang Y, Wei S, Nie S (2014) Application of a new hybrid model with seasonal auto-regressive integrated moving average (ARIMA) and nonlinear auto-regressive neural network (NARNN) in forecasting incidence cases of HFMD in Shenzhen, China. *PloS one* 9(6):e98241